

VU Research Portal

Novel prognostic biomarkers in head and neck cancer

Mes, S.W.

2021

document version

Publisher's PDF, also known as Version of record

[Link to publication in VU Research Portal](#)

citation for published version (APA)

Mes, S. W. (2021). *Novel prognostic biomarkers in head and neck cancer*. [PhD-Thesis - Research and graduation internal, Vrije Universiteit Amsterdam].

General rights

Copyright and moral rights for the publications made accessible in the public portal are retained by the authors and/or other copyright owners and it is a condition of accessing publications that users recognise and abide by the legal requirements associated with these rights.

- Users may download and print one copy of any publication from the public portal for the purpose of private study or research.
- You may not further distribute the material or use it for any profit-making activity or commercial gain
- You may freely distribute the URL identifying the publication in the public portal ?

Take down policy

If you believe that this document breaches copyright please contact us providing details, and we will remove access to the work immediately and investigate your claim.

E-mail address:

vuresearchportal.ub@vu.nl



3

Prognostic modeling of oral cancer by gene profiles and clinicopathological co-variables

Steven W. Mes*, Dennis te Beest*, Tito Poli, Silvia Rossi,
Kathrin Scheckenbach, Wessel N. van Wieringen,
Arjen Brink, Nicoletta Bertani, Davide Lanfranco,
Enrico M. Silini, Paul J. van Diest, Elisabeth Bloemena,
C. René Leemans, Mark A. van de Wiel*, Ruud H. Brakenhoff*

**These authors have contributed equally to this work.*

Oncotarget 2017; 8(35): 59312-23

ABSTRACT

Accurate staging and outcome prediction is a major problem in clinical management of oral cancer patients, hampering high precision treatment and adjuvant therapy planning. Here, we have built and validated multivariable models that integrate gene signatures with clinical and pathological variables to improve staging and survival prediction of patients with oral squamous cell carcinoma (OSCC). Gene expression profiles from 249 human papillomavirus (HPV)-negative OSCCs were explored to identify a 22-gene lymph node metastasis signature (LNMsig) and a 40-gene overall survival signature (OSsig). To facilitate future clinical implementation and increase performance, these signatures were transferred to quantitative polymerase chain reaction (qPCR) assays and validated in an independent cohort of 125 HPV-negative tumors. When applied in the clinically relevant subgroup of early-stage (cT1-2N0) OSCC, the LNMsig could prevent overtreatment in two-third of the patients. Additionally, the integration of RT-qPCR gene signatures with clinical and pathological variables provided accurate prognostic models for oral cancer, strongly outperforming TNM. Finally, the OSsig gene signature identified a subpopulation of patients, currently considered at low-risk for disease-related survival, who showed an unexpected poor prognosis. These well-validated models will assist in personalizing primary treatment with respect to neck dissection and adjuvant therapies.

INTRODUCTION

Head and neck squamous cell carcinoma (HNSCC) is the 7th most common tumor in the world¹. HNSCC originates in the mucosal linings of the oral cavity, oropharynx, hypopharynx and larynx. The majority of patients (30-40%) present with oral squamous cell carcinoma (OSCC)². Classical risk factors for HNSCC are tobacco use and alcohol consumption. Additionally, human papillomavirus (HPV) infection became manifest as a cause during the last decade. The HPV-attributable fraction is highest in oropharyngeal squamous cell carcinoma (OPSCC), and varies from 20-90% depending on the geographical region³. Also oral cancers may arise from HPV infection, but the attributable fraction is lower, ranging from 0-6%⁴. OPSCCs caused by HPV infection are different at the molecular level⁵ and have a highly favorable prognosis⁶. This different clinical behavior led to treatment de-intensifying trials to personalize treatment and a staging adaptation in the 8th edition of the TNM Classification of Malignant Tumors of the Union for International Cancer Control (UICC)⁷.

The 5-years overall survival for OSCC is 60%, but ranges from 10 to 80% depending on the extent of the tumor at diagnosis⁸, as defined by the TNM stage. TNM staging is based on prognosis and employed for treatment planning in patients with OSCC⁹, but is group-based and meets limitations for personalizing treatment of the individual patient.

OSCC is mainly treated by surgery with or without postoperative radiotherapy or chemoradiotherapy, and besides TNM stage, additional important prognostic features are derived from histopathological examination of the surgical specimen. For example, tumor-positive surgical margins (R+) and lymph node metastasis (LNM) with extracapsular spread (ECS) are classical treatment-decisive prognostic factors and indicators for postoperative chemoradiotherapy. Of note, histopathological examination of the specimen is only available for postoperative therapy decisions, and not for pre-treatment prediction of prognosis and treatment planning. Particularly for patients with a clinically N0 neck an important choice has to be made between elective treatment of the neck, with associated morbidity, or active surveillance with the risk of occult lymph node metastases that will become manifest during follow-up. Molecular profiling of tumor specimen may provide additional, objective information to improve current prognostication, and can even be performed on pretreatment biopsies to stage the neck.

Several prognostic models based on molecular profiles have been evaluated for HNSCC in general, or for OSCC specifically¹⁰⁻¹³. These models predicted survival of the studied populations, and added independent information to other established prognostic factors. However, none of these models has been introduced in clinical practice. Reasons are (1) insufficient clinical validation of the models, (2) the complexity and lack of reproducibility of the different profiling platforms¹⁴, (3) heterogeneous study populations regarding HPV status and tumor subsite, (4) the high costs of transcriptomic profiling, and (5) the lack of compatibility with formalin-fixed paraffin-embedded (FFPE) tissue specimen. Translation of expression profiles to quantitative real-time polymerase chain reaction (qPCR) platforms using selected gene panels may overcome most of these disadvantages.

Another argument holds true for expression profiles associated with the clinically N0 neck. Previously, an expression profile has been identified and appropriately validated in a multicenter trial¹⁵⁻¹⁷. The signature remained accurate with negative predictive values (NPV) of 88% to 90% in the clinically relevant subgroup. However, the sentinel node biopsy is a competing diagnostic modality in this patient group with an even higher NPV of 95%¹⁸. Notwithstanding, sentinel node biopsy has not been introduced widely, has a poor performance for floor of mouth tumors, and has the obvious disadvantage that it remains a surgical procedure with radioactive tracers, whereas for gene expression analysis only a biopsy is required. Particularly, switching to RT-qPCR analysis of a thoroughly selected gene panel may further enhance the predictive power of the gene signature because of the large dynamic range of RT-qPCR.

We therefore aimed to identify and test gene expression signatures to address these important challenges in head and neck oncology: prediction of lymph node metastasis (LNM) and overall survival (OS). First, signatures of informative genes were selected from gene expression data by regression methods. Next, a limited number of genes were selected for platform transition to RT-qPCR assays, and the prognostic power was validated

using an independent cohort of surgically-treated HPV-negative OSCC patients. The molecular data were further combined with clinical and pathology data to provide the most accurate models for clinical practice to predict nodal metastatic disease and prognosis.

MATERIALS AND METHODS

Patients

Four independent cohorts of human papillomavirus (HPV)-negative OSCC patients were included (1) a cohort of 2 merged tumor gene expression profiles (array cohort 1, AC1) from the University Medical Center Utrecht (UMCU) and VU University Medical Center Amsterdam (VUmc); (2) a cohort of tumor gene expression profiles (array cohort 2, AC2) from the University Hospital Parma Medical Center (UHPMC); (3) an independent cohort of frozen tumor samples from VUmc, UHPMC and University Hospital Düsseldorf (UHD) for RT-qPCR gene expression profiling (qPCR cohort); and (4) an RNAseq dataset of OSCC tumors from The Cancer Genome Atlas (TCGA) Network¹⁹. Use of tissue from surgical specimen adhered to nation- and institution-specific procedures and guidelines. Informed consent was obtained of enrolled patients, when required. This study followed the Guidelines for the REporting of tumor MARKer Studies (REMARK)²⁰ (Supplementary Table 6).

HPV status

HPV status was either determined with p16 immunostaining followed by HPV DNA PCR on p16-positive samples (AC1) and/or with HPV16 E6*I RT-PCR in the AC1 and qPCR cohorts. Both assays have been validated and described before²¹. In AC2, the HPV status was not available. In the other cohorts on the other hand, 1 out of 151 (AC1) and 1 out of 126 (qPCR cohort) tumors were HPV-positive. Hence, the contribution of HPV positive tumors in AC2 was assumed to be low and no samples were excluded.

Gene expression datasets

Similarly preprocessed VUmc (GSE84846) and UMCU (GSE30788) microarray datasets were combined, and comparability of the expression data of both centers was ensured. Data from AC2 (GSE84846) were not combined to the other datasets, because of a different reference design: Universal Human Reference RNA (cat. 740000, Agilent Technologies, Santa Clara, CA, USA) in AC1 and a pool of cell line RNA in AC2 (CAL 27, ATCC CRL-2095, American Type Culture Collection, Manassas, VA, USA). All preprocessing steps of the microarray data were performed using the limma package²² in R (Supplementary Materials).

RT-qPCR

RNA was purified from fresh frozen tumor tissue and synthesis of cDNA was performed from 1 µg of total RNA using the High-Capacity RNA-to-cDNA Kit (cat. 4387406, Applied Biosystems; Foster City, CA). qPCR was performed using Taqman Low-Density Array (TLDA) Cards (cat. 4346800, Applied Biosystems) (Supplementary Table 2). qPCR Ct values were determined with predefined thresholds that were equal per gene for all patients. Relative gene expression was determined by the $\Delta\Delta C_t$ method²³ using GUSB Ct-values for normalization. GUSB was selected as the most stable housekeeping gene (see Supplementary Table 7) out of four candidate genes (GAPDH, GUSB, RPLP0, and RPL4).

Statistical analyses

Per dataset, the predictive power for LNM and survival was assessed with the global test^{24,25}. Datasets with significant predictive power ($p < 0.05$) were used for gene selection. Genes were selected from the microarray data by using a combination (detailed later) of lasso logistic regression or lasso Cox regression and univariable FDR-based association analysis. The latter was included to enhance reproducibility of individual markers assayed

by qPCR. The gene selection procedure is displayed in Figure 1 and further detailed in the Supplementary Materials. For the LNM genes, the p-values per gene of AC1 and AC2 were combined by Fisher's combined probability test, whereas for the prognostic genes only p-values of AC1 were considered, because the AC2 data did not pass the global test. For technical validation, the correlation between microarray and RT-qPCR data of 20 cases was determined by Pearson's correlation coefficient. For the RT-qPCR data, the univariable association of delta Ct values of the selected genes with either LNM or OS was determined by logistic or Cox regression, respectively. For prediction on independent samples, clinical variables were selected using stepwise regression, followed by adding the selected genes in a logistic (Cox) ridge regression to render multi-type prediction models. Model performance was assessed by bootstrapping. The prediction models for outcome consisted of (1) prognostic genes, (2) significant clinical factors and pathological TNM-stage (pTNM), (3) significant clinical factors and a composite pathological variable (positive if ECS or R+ surgical margins or >1 LNM was present), and the combinations (4) 1+2 and (5) 1+3. The predictive performance was assessed by area-under-the-ROC-curve (AUC) and integrated AUC (iAUC) over 5-year follow-up time for LNM and OS, respectively, complemented for LNM by the negative predictive value (NPV). Additive value of the gene signature was assessed with the global test. All statistical tests performed were two-sided. Univariable p-values were corrected for multiple testing using the Benjamini-Hochberg FDR procedure²⁶.

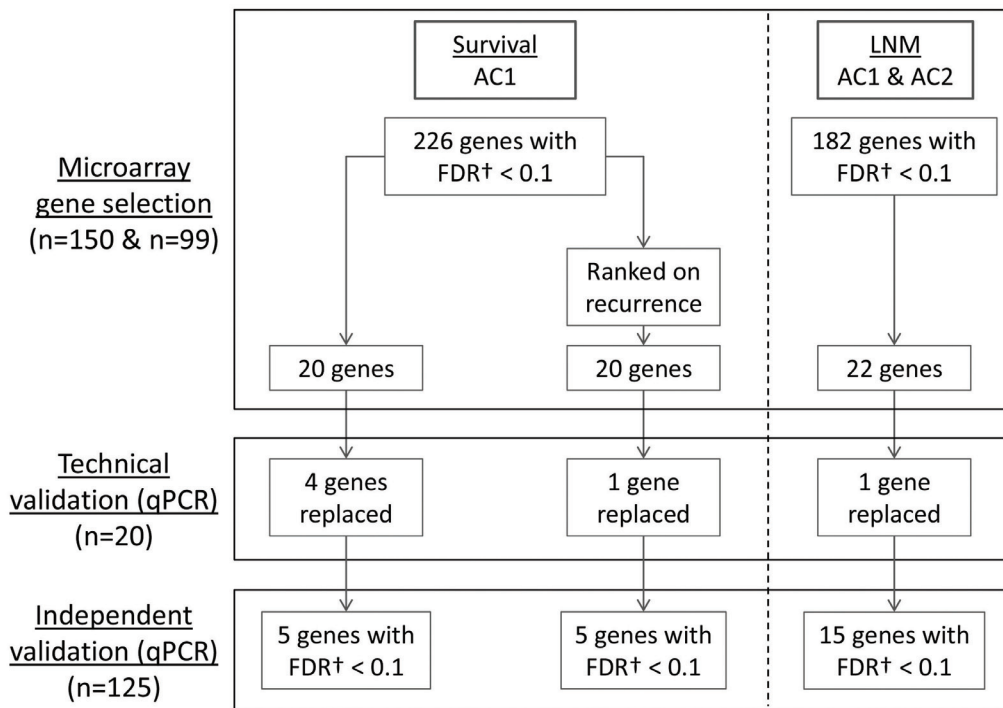


Figure 1. Schematic representation of the different phases of the study.

Two microarray cohorts (Array Cohort 1 (AC1), n=150; Array Cohort 2 (AC2), n=99) were explored by univariable and multivariable gene selection to identify a 22-gene lymph node metastasis signature (LNMsig) and a 40-gene overall survival signature (OSsig). For the OStsig, 20 genes were selected that were predictive for OS, and 20 additional genes were selected after the genes were ranked on their predictive value for recurrent disease to account for disease-specific death. For LNM prediction, a previously validated multigene microarray signature (15–17) was used as preselection. Subsequently, our signatures were transferred to RT-qPCR assays and correlated to the microarray data in 20 cases (technical validation). After this technical validation, 6 genes with poor correlation coefficients were replaced by the second best genes from the initial microarray analyses. Finally, the definitive signatures were validated on an independent cohort of 125 tumors (independent validation). †Univariable p-values were corrected for multiple testing using the Benjamini-Hochberg FDR procedure. AC1, Array Cohort 1; AC2, Array Cohort 2; FDR, false discovery rate; LNM, lymph node metastasis; qPCR, quantitative polymerase chain reaction.

RESULTS

Microarray data from two cohorts, 150 OSCC patients from The Netherlands (Array Cohort 1, AC1) and 99 OSCC patients from Italy (Array Cohort 2, AC2), were used to identify genes related to LNM and OS (Table 1). LNM was present in 60% of AC1 patients and 49.5% of AC2 patients. In AC1, the median overall follow-up time was 7.2 years (95% CI = 6.7 – 8.1). In AC2, the median overall follow-up time was 3.5 years (95% CI = 3.3 – 4.3).

Table 1. Characteristics of Patients in the Four Study Cohorts^a

Characteristic	Array Cohort 1 (n = 150)	Array Cohort 2 (n = 99)	qPCR Cohort (n = 125)	TCGA Cohort (n = 160)	P ^b Value
Age, mean (SD)	62 (10.7)	66 (10.3)	63 (12.6)	62 (13.6)	P=0.06
Gender					
Male (%)	90 (60.0)	54 (54.5)	72 (57.6)	105 (65.6)	P=0.30
Female (%)	60 (40.0)	45 (45.5)	53 (42.2)	55 (34.4)	
Smoking (PY)					
0-10 (%)	36 (24.0)	51 (51.5)	41 (32.8)	47 (29.4)	P<0.001
11-24 (%)	19 (12.7)	10 (10.1)	13 (10.4)	13 (8.1)	
>24 (%)	95 (63.3)	38 (38.4)	71 (56.8)	60 (37.5)	
Unknown (%)	-	-	-	40 (25.0)	
Subsite					
Oral tongue (%)	53 (35.3)	41 (41.4)	48 (38.4)	-	P=0.62
Other oral cavity (%)	97 (64.7)	58 (58.6)	77 (61.6)	-	
TNM stage					
I (%)	18 (12.0)	22 (22.2)	16 (12.8)	10 (6.3)	P=0.02
II (%)	22 (14.7)	12 (12.1)	27 (21.6)	32 (20.0)	
III (%)	31 (20.7)	21 (21.2)	26 (20.8)	25 (15.6)	
IV (%)	79 (52.7)	44 (44.4)	56 (44.8)	82 (51.3)	
Unknown (%)	-	-	-	11 (6.9)	
N-stage					
Negative (%)	60 (40)	48 (48.5)	61 (48.8)	57 (35.6)	P=0.35
Positive (%)	90 (60)	49 (49.5)	64 (51.2)	76 (47.5)	
Unknown	-	2 (2.0)	-	27 (16.9)	
pCompVar ^c					
Negative (%)	-	-	79 (63.2)	-	
Positive (%)	-	-	38 (30.4)	-	
Unknown (%)	-	-	8 (6.4)	-	

Abbreviation: pCompVar, pathological composite variable; PY, packyears; SD, standard deviation.

^a Percentages may not total 100 because of rounding.

^b P values were calculated with the use of One-Way ANOVA for continuous variables and χ^2 test for categorical variables.

^c Scored positive if extracapsular spread or positive resection margins or >1 lymph node metastasis was present.

Identification of genes for prediction of lymph node metastasis and survival in OSCC

The gene selection strategy is summarized in Figure 1 and described in detail in the Supplementary Materials. In short, the previously published LNM gene profile^{15,17} was evaluated to predict N-stage in AC1 and AC2. Using the global test with pathological N-stage as outcome, these genes had a p-value of 9.3E-06 and 9.9E-03 in AC1 and AC2, respectively. Combined univariable analysis identified 221 significant genes (FDR<0.1, Supplementary Table 1). From these genes, 22 genes were selected for RT-qPCR validation based on their ranking in univariable and multivariable analysis.

For survival, a similar gene pre-selection strategy was hampered by the lack of thoroughly validated prognostic gene signatures in the public domain. We therefore included other techniques to reduce the dimensions of the data, but also explored all genes to ensure that important prognostic genes were not missed. We only used AC1 for gene selections, as AC2 did not pass the global test due to the shorter follow-up time (global test

p-values AC1: 7.8E-3 and AC2: 0.73). Univariable analysis of all genes identified 226 (out of 37,662) significant genes in AC1 (FDR<0.1, Supplementary Table 1). Next, 20 genes were selected by univariable and multivariable analyses for survival, and 20 additional genes were selected after ranking the genes on their predictive value for recurrent disease to account for disease-specific death (see Figure 1). Two genes overlapped between the 40 survival genes and the 22 LNM genes (Supplementary Figure 1), rendering an overall signature of 60 target genes for technical and independent RT-qPCR validation (Supplementary Table 2).

Technical RT-qPCR validation of identified genes

First, the 60 target genes were technically validated in a subset of 20 cases from AC2 to evaluate the platform transition. For these 20 cases, correlation coefficients were calculated between microarray and corresponding RT-qPCR data (Supplementary Table 3). In total, 52 of 60 genes validated well, as they showed a good correlation between microarray and RT-qPCR data (mean $r=0.64$, $SD=0.26$). The remaining 8 genes correlated poorly, showing a correlation coefficient >1 SD below the mean. Cox regression nonetheless indicated that two of these eight genes did correlate with survival, i.e. EIF5 ($P=0.011$) and ATP6V0A1 ($P=0.057$), and these were therefore kept in the panel. The remaining 6 genes were replaced by the second best genes from the initial microarray analyses (Supplementary Table 1), and subsequently analyzed.

Independent RT-qPCR validation of selected genes

The RT-qPCR validation cohort consisted of 125 OSCC cases that were independent from both microarray cohorts. In this validation cohort, nodal metastasis was detected in 51.2% of patients, and the median overall follow-up time was 5.1 years (95% CI = 4.4 – 6.3) (Table 1). The selected genes were run on customized microfluidic RT-qPCR cards, and the results were tested by univariable analyses and corrected for multiple testing. From the LNMsig 15 of 22 genes had an FDR<0.1 (Supplementary Table 4). From the OSSig 10 of 40 genes had an FDR<0.1 for OS, seven of which also significantly associated with disease-free survival (DFS). Thus, after correction for multiple testing, in total 25 of 60 genes selected from microarray datasets could be validated with RT-qPCR assays in an independent patient cohort.

Table 2. Performance Metrics of Gene Signature in N-stage prediction

	qPCR validation, all (n = 125)	qPCR validation, cT1-2N0 (n = 54)
NPV (95% CI ^a)	66 (57.1-74.7)	84 (71.7-95.2)
TN	40	26
TN + FN	61	31
PPV (95% CI ^a)	67 (59.1-76.6)	43 (21.5-64.5)
TP	43	10
TP + FP	64	23
Sensitivity (95% CI ^a)	67 (42.3-83.5)	67 (29.6-93.2)
TP	43	10
TP + FN	64	15
Specificity (95% CI ^a)	66 (39.3-83.2)	67 (39.7-86.2)
TN	40	26
TN + FP	61	39
AUC (95% CI ^a)	0.69 (0.63-0.75)	0.66 (0.52-0.78)

Abbreviations: AUC, Area Under the ROC Curve; CI, confidence interval; FN, false negative; FP, false positive; NPV, negative predictive value; PPV, positive predictive value; TN, true negative; TP, true positive.

^a. Confidence intervals were assessed by bootstrapping.

A gene expression-based model to predict lymph node metastasis in OSCC

The performance of the LNM predictive signature is summarized in Table 2; see Supplementary Table 4 for the estimates per gene. When all clinical stages of disease are considered, the AUC of this model was 0.69 (Table 2), with an NPV of 66% (Table 2). Next, we performed a subgroup analysis on the clinically relevant subset of tumors with clinical stages I and II ($n=54$), because these tumors qualify for transoral resection without treatment of the neck. In this subgroup, the AUC (0.66, Table 2) and the sensitivity of the LNMsig (67%, Table 2) were comparable with the performance statistics in all stages. The NPV, however, increased from 66% to 84% (Table 2). There were no clinical variables that correlated to LNM (data not shown) and data from histopathology is not available before surgery planning. Moreover, the fraction of occult lymph node metastasis was comparable in cT1 and cT2 tumors (i.e. 25% and 29% respectively). Previously, Van Hooff et al.¹⁷ proposed a clinical decision model that recommends an elective neck dissection when the gene expression signature prediction indicates N+ or active surveillance when the prediction is N0, and estimated the benefit. Following this decision model, the LNMsig shows a similar benefit and could have prevented overtreatment in over 66% of the pN0 cases (72% or 24% overtreatment without or with the clinical decision model, respectively; see Figure 2).

A gene expression-based prognostic model for OSCC with independent prognostic value

The 40 survival genes significantly discriminated between high and low risk cases (OS: $iAUC=0.63$, $P=1.6E-3$ (global test), Table 3 and Figure 3A-left; DFS: $iAUC=0.65$, $P=6.8E-3$ (global test), Table 3 and Figure 3A-right; see Supplementary Table 4 for Ridge estimates per gene). In a clinical setting the genes should add prognostic information to established parameters. Hence, the gene signature was analyzed in context of clinical and histopathological data.

Several clinical factors were associated with OS, and none with DFS. A model was trained with the most important clinical factors for this dataset and pathological TNM-stage (pTNM). The clinical factors selected and included in the model were: age at diagnosis and smoking (i.e. packyears, PY), see Supplementary Table 5 for univariable p-values. The model with these two clinical factors and pTNM accurately predicted overall survival ($iAUC=0.66$, Table 3), but not DFS ($iAUC=0.53$, Table 3). Adding OSSig to this model improved the accuracy (OS: $iAUC=0.68$, OSSig: $P=0.03$ (global test), Table 3 and Supplementary Figure 2A). For DFS, a model based on the two clinical variables + pTNM and the OSSig gave an $iAUC$ of 0.60. Note that this is lower than a model based on the OSSig only ($iAUC$ 0.65).

Besides pTNM, other histopathological variables are important to decide on adjuvant treatment. In the Dutch guidelines, decisive criteria for adjuvant postoperative therapy are extracapsular spread (ECS), tumor-positive margins (R+) and multiple metastatic lymph nodes (>1 LNM). We created a composite variable (pCompVar) that was scored positive if ECS or R+ or >1 LNM was present. This composite variable was combined with clinical factors (i.e. age, PY) in a prognostic model (OS: $iAUC=0.73$, DFS: $iAUC=0.62$; see Table 3). The OSSig improved the accuracy of the model (OS: $iAUC=0.74$, OSSig: $P=0.02$ (global test), Table 3 and Supplementary Figure 2B; DFS: $iAUC=0.68$, OSSig: $P=0.01$ (global test), Table 3). DFS was most accurately predicted by a model that combined the OSSig and pCompVar, not including pTNM ($iAUC=0.70$; OSSig: $P=5.6E-3$ (global test)).

A subgroup analysis was performed with patients without criteria for postoperative radiotherapy, i.e. cases that were pCompVar-negative ($n=79$, Figure 3B-left). For these cases a multi-type prognostic model was built that included clinical factors (age and smoking) and the OSSig. The $iAUC$ increased from 0.70 to 0.73 by adding the prognostic genes (Table 3 and Figure 3B-right). Predictive models for DFS were less accurate in this subgroup, although a predictive model with genes only showed some predictive power ($iAUC=0.65$, OSSig: $P=0.27$) (Supplementary Figure 3, Supplementary Table 3).

These findings show that the prognostic value of the OSSig adds to established clinical and pathological prognostic variables.

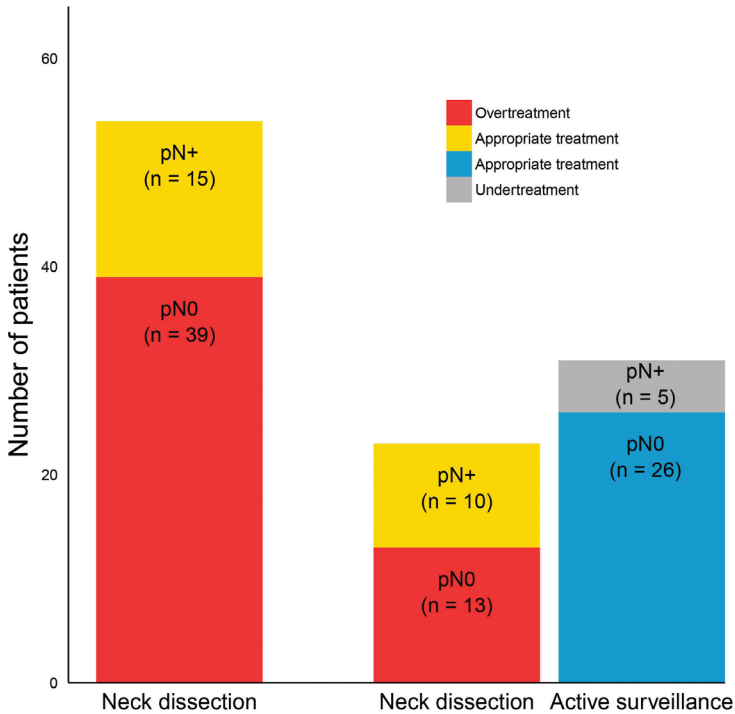


Figure 2. Incorporation of the LNMsig in a clinical decision model that was previously proposed for patients with clinically early stage (cT1-T2N0) oral squamous cell carcinoma (OSCC).

At present, early-stage OSCCs are treated with an elective neck dissection (END, levels I-III or I-IV depending on location) in most centers. This would cause overtreatment in 39 patients (first bar, indicated in red). The clinical decision model recommends performing an END when the gene expression signature prediction is N+ or active surveillance when the prediction is N0. The hypothetical situation when using this decision model is represented in the second and third bar. Following the decision model, only 23 patients are directly treated with an elective neck dissection (second bar), overtreatment is restricted to 13 cases, and 26 patients receive appropriate treatment (third bar). The patients who are pN+ and receive an END are labeled as receiving appropriate treatment (indicated by yellow color).

External validation of LNMsig and OSSig with TCGA RNAseq data

For additional external validation, we used RNAseq data of HPV-negative OSCC tumors from the TCGA Network publication¹⁹ (n=160, Table 1). The 22-gene LNMsig was significantly associated to pathological N-stage ($P = 7.6E-06$, global test). Moreover, the LNMsig could accurately classify the tumors with an AUC of 0.73 (95% CI = 0.67 to 0.78). The performance of the 40-gene OSSig was also significant (iAUC=0.59, $P=0.02$ (global test), Supplementary Figure 4). The OSSig was less informative since the average follow-up time for the 89 non-deceased cases was very short (2.2 years, SD = 2.35, Supplementary Figure 5A), and the baseline hazard was relatively high when compared to the RT-qPCR validation cohort (Supplementary Figure 5B).

Table 3. Univariable and multivariable analysis of genomic, clinical, pathological and combined models in validation cohort

	Overall survival iAUC^a (95% CI^b)	P^c value	Disease free survival iAUC^a (95% CI^b)	P^c value
Unitype				
OSsig	0.63 (0.57-0.68)	0.002	0.65 (0.60-0.70)	0.007
Clinical	0.66 (0.59-0.73)		0.54 (0.49-0.61)	
pTNM	0.51 (0.47-0.57)		0.51 (0.47-0.57)	
pCompVar ^d	0.64 (0.56-0.71)		0.63 (0.56-0.71)	
Multitype				
Clinical+pTNM	0.66 (0.60-0.73)		0.53 (0.47-0.60)	
OSsig+clinical+pTNM	0.68 (0.64-0.73)	0.03	0.60 (0.55-0.64)	0.01
Clinical+pCompVar ^d	0.73 (0.67-0.80)		0.62 (0.54-0.70)	
OSsig+clinical+pCompVar ^d	0.74 (0.69-0.79)	0.02	0.68 (0.63-0.73)	0.01
pCompVar ^d negative subgroup				
OSsig	0.71 (0.65-0.76)	0.01	0.65 (0.61-0.68)	0.28
Clinical	0.70 (0.61-0.79)		0.53 (0.43-0.68)	
OSsig+clinical	0.73 (0.68-0.78)	0.02	0.52 (0.46-0.65)	0.47

Abbreviations: iAUC, integrated Area Under the Curve; OSsig, Overall Survival signature; pCompVar, pathological composite variable; pTNM, pathological TNM stage

^a Area under the curve was integrated over 5 year follow-up time.

^b CIs were assessed by bootstrapping on out-of-bag samples.

^c Significance of the OSsig was assessed with the global test^{22,23}.

^d Scored positive if extracapsular spread or positive resection margins or >1 lymph node metastasis was present.

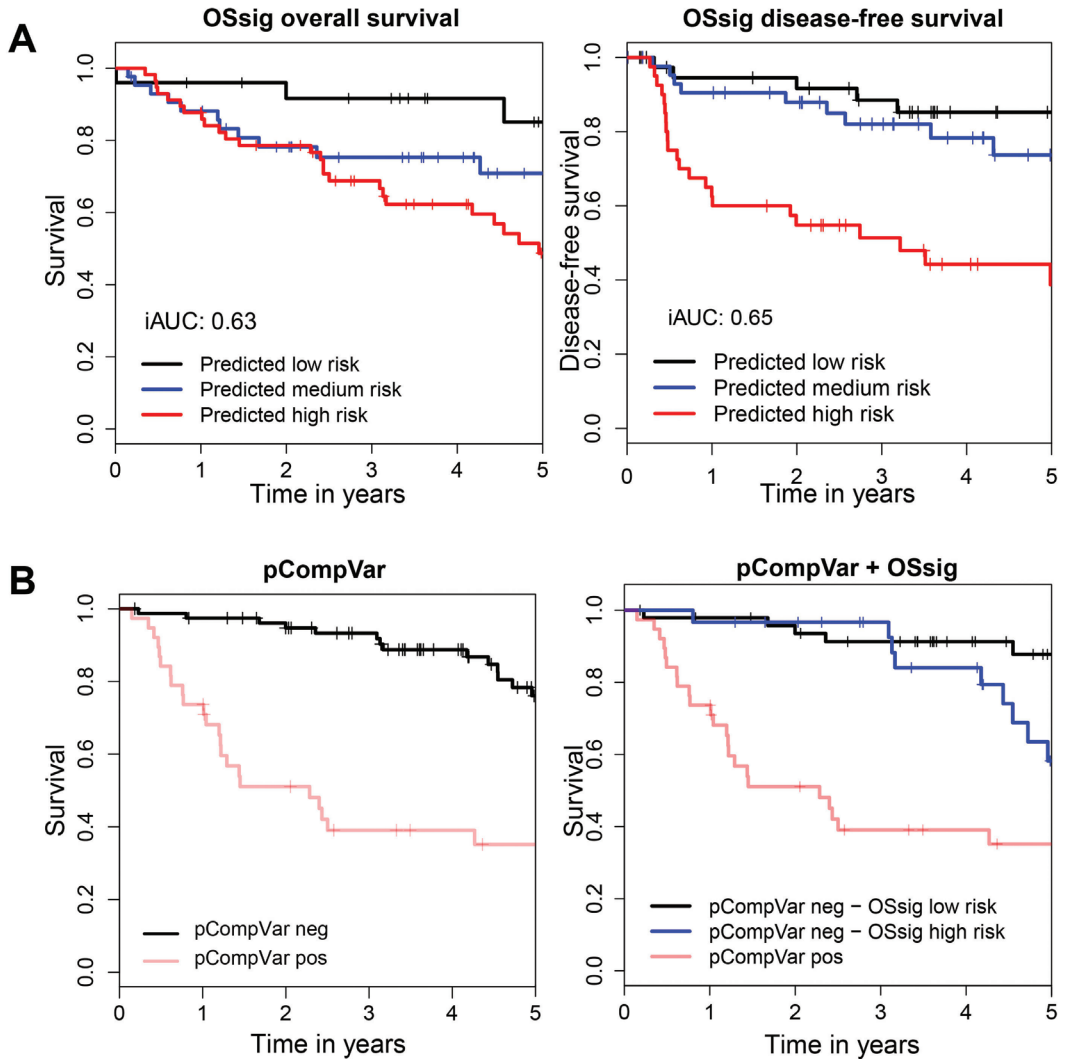


Figure 3. The overall survival signature (OSsig) predicts overall survival and disease-free survival, also in low-risk patients.

(A) Kaplan-Meier analysis of overall survival (left) and disease-free survival (right) with risk groups defined by tertile predicted hazards by the OSsig analyzed with qPCR in the independent validation cohort of 125 OSCC patients. We also considered threshold optimization for creating the three groups; resulting KM curves were very similar and are hence not displayed. (B) On the left, a Kaplan-Meier analysis is shown for overall survival in the independent validation group with risk groups defined by pCompVar, which is scored positive when during histopathological examination either extracapsular spread (ECS) or involved resection margins (R+) or >1 lymph node metastasis was identified. These are routinely used histopathological criteria for adjuvant treatment. On the right the result of a subgroup analysis is shown to improve the stratification of the pCompVar-negative patients ($n=79$). TNM-staging was not informative to stratify this group (data not shown), but the OSsig was able to identify a subgroup of patients (blue line) with relatively poor prognosis who might have benefited from adjuvant treatment (OS: iAUC=0.71; OSsig: $P=0.01$ (global test)). The performances of all predicting models are listed in Table 3. Area under the curve was integrated over 5 year follow-up time. Tick marks on curves indicate censoring. iAUC, integrated Area Under the Curve; OSsig, Overall Survival signature; pCompVar, pathological composite variable.

DISCUSSION

We identified prognostic gene expression signatures that are predictive of LNM and OS in OSCC by rigorous gene selection and validation. First, we selected 60 genes using microarray data, and these genes were validated in an independent cohort of OSCC patients by the use of RT-qPCR assays. Finally, we built 2 multivariable genomic models: a lymph node metastasis model (LNMsig) and overall survival model (OSsig) and confirmed the additive value of the gene signatures to existing and established variables.

The LNMsig with 22 genes predicted nodal metastatic disease with an NPV of 84% in clinical stages I and II. These diagnostic performance statistics are comparable to previous results using a 732-probe microarray signature¹⁷. However, the RT-qPCR approach facilitates clinical implementation considerably, because a comparable performance was achieved with less genes and a more user-friendly platform. A high NPV is necessary to identify patients who can be spared an elective neck dissection. Recent reports showed that the sentinel node biopsy (SNB), which is an alternative staging technique, is more accurate with an NPV of 95%¹⁸ at comparable prevalence rates of LNM. The SNB, however, is an invasive surgical procedure with associated risks and costs, and with lower sensitivity in floor of mouth tumors²⁷⁻²⁹. Moreover, it has not been introduced widely. It has been suggested that a combination of an expression signature and SNB may be more accurate for staging of the clinically N0 neck³⁰.

The OSsig could be used to personalize treatment. By itself, the OSsig predicted overall survival with an iAUC of 0.63, which is already promising compared to the iAUC of 0.51 of standard pTNM. For prediction of DFS, the OSsig was even more valuable, particularly when combined with histopathology, as clinical variables were not informative for DFS. These data confirm the predictive value of the OSsig, but also indicate that integrating clinical, molecular and histopathological variables delivers most accurate predictive models.

The design of this study enabled the identification of robust associations in three ways. First, we used different gene expression platforms to cancel out platform-specific findings. Second, we studied homogeneous patient cohorts: only HPV-negative, surgically treated OSCCs were included. Finally, we considered patients from 3 European countries, thereby excluding the discovery of population-specific gene signatures.

Our findings may be limited by two factors. First, intra-tumor heterogeneity may cause differences in gene expression profiles within a tumor; although previous findings suggest that expression profiles seem stable in HNSCC³¹. Second, all cohorts investigated were retrospective. It should be mentioned, however, that retrospective data obtained in The Netherlands are generally accurate, because treatment and follow-up of HNSCC patients has been centralized to a few clinical centers and clinical management adheres to standardized national guidelines.

Our findings suggest at least two implications. First, the prognostic model may be used for treatment escalation in patients with tumors that do not fulfill the current criteria for postoperative radiotherapy, i.e. margin involvement, >1 metastatic lymph node or ECS. Second, a model that integrates clinical variables and the OSsig accurately predicts prognosis without the addition of histopathology. This model may specifically be important to predict survival in patients who are treated with primary radiotherapy or chemoradiotherapy, since histopathology is not available for these patients. These are important directions for future work. Since frozen material is not always available in these cases, future research should also include applications for FFPE tissue. Ultimately, prospective clinical trials will be required to determine whether the integrated risk models could guide clinical decision making and improve treatment results with respect to outcome and morbidity.

ACKNOWLEDGEMENTS

We thank V. Okpanyi and L. Colter for sample preparation and assembly of clinical data; F. Rustenburg, P. Eijk, S. Smeets and B. Ylstra for processing of the VUmc microarrays; Agendia for making the UMCU data available; M.

Doeleman and D. Heideman for the E6*I RT-PCR HPV testing; and A. Visser and C. Oudejans for their assistance with the qPCR microfluidic cards.

CONFLICTS OF INTEREST

The authors have declared that no conflicts of interest exists.

FUNDING

This work was supported by grants from the Dutch Cancer Society, KWF (grant number 2008-4201) and European Union's Seventh Framework Project (grant agreement 224483: NeoMark, and grant agreement 611425: OraMod).

SUPPLEMENTARY METHODS

Patients

Four independent cohorts of oral squamous cell carcinoma (OSCC) patients with frozen biopsies were included in this study: (1) a cohort of 150 patients from the University Medical Center Utrecht (UMCU) and VU University Medical Center Amsterdam (VUMC) for microarray gene expression profiling (array cohort 1, AC1); (2) a cohort of 99 patients from the University Hospital Parma Medical Center (UHPMC) for microarray gene expression profiling (array cohort 2, AC2); (3) a cohort of 125 patients from VUMC, UHPMC and University Hospital Düsseldorf (UHD) for qPCR gene expression profiling; and (4) an RNAseq dataset of HPV-negative OSCC tumors from the Cancer Genome Atlas Network publication¹⁹. Inclusion criteria were: presentation with a squamous cell carcinoma in the oral cavity, date of incidence prior to July 1st 2012, and treated surgically with curative intent. All patients were 18 years or older and had no previous malignancy that impacts outcome. Included ICD-10 codes were: C00.3-4, C02.0-3, C02.8-9, C03, C04, C05.0, and C06. Human papilloma virus (HPV) positive tumors were excluded from further analysis. Informed consent was obtained of enrolled patients when required, and nation- and institution-specific procedures and guidelines were followed in addition. For instance, for the Netherlands use of residual tissue from surgical specimen adhered to the Code of conduct for responsible use by the Federation of Dutch Medical Scientific Societies (FDMSS). This study followed the Guidelines for the REporting of tumor MARKer Studies (REMARK)²⁰ (Supplementary Table 6).

Specimen

Biopsies were taken from the surgical specimen at time of surgery, snap frozen and subsequently stored in liquid nitrogen. Five to ten 20 µm sections were used for RNA isolation. Before and after sampling of the 20 µm sections, 5 µm sections were made and stained by haematoxylin and eosin to ensure that at least 50% tumor cells were present in the biopsy. RNA isolation was performed using TRIzol (cat. 15596026, Life Technologies, Breda, The Netherlands; AC1) or with columns using the RNeasy Mini Kit (cat. 74104, Qiagen, Hilden, Germany; AC2 and qPCR cohort), according to the protocol of the suppliers. HPV status was either determined with p16 immunostaining followed by HPV DNA PCR on p16-positive samples (AC1) or with HPV16 E6*I RT-PCR (qPCR cohort) in the AC1 and AC3 cohorts. Both assays have been validated and described before²¹. In AC2, the HPV status was not determined. In the other cohorts on the other hand, 1 out of 151 (AC1) and 1 out of 126 (qPCR cohort) tumors were HPV-positive. Hence, the contribution of HPV positive tumors in AC2 was assumed low and no further samples were excluded. Quantity and quality of the RNA was tested with the Nanodrop (cat. ND-1000, Thermo Fisher Scientific, Amsterdam, The Netherlands) and the Bioanalyzer 2100 (cat. G2939AA, Agilent Technologies, Amstelveen, The Netherlands) using the RNA Nanokit (cat. 5067-1511, Agilent). RNA Integrity Numbers (RIN-value) were between 6.3 and 10.0.

Expression arrays

Two independent cohorts of OSCC patients were processed for gene expression microarray analysis: (1) a cohort of 2 merged tumor gene expression profiles (array cohort 1, AC1); and (2) array cohort 2 from the University Hospital Parma Medical Center (UHPMC). In AC1, array hybridization was performed, using 0.5 µg total RNA in the Low RNA Input Linear Amplification Kit (cat. 5184-3523, Agilent) and the 4x44K Whole Human Genome Arrays, according to the manufacturer (Agilent) using dual color labeling. The handling of the UMCU samples and their RNA isolation has been published before¹⁷. Microarray data of UMCU were retrieved from the Gene Expression Omnibus (GSE30788). Additional information on these samples was obtained from Agendia (Amsterdam, the Netherlands). In AC2, 0.2 µg of total RNA was labeled and simultaneously amplified following the “Two-Color Microarray-Based Gene Expression Analysis (Quick Amp Labeling) Protocol” (Agilent Technologies). Labeled-amplified RNA samples were then hybridized on 4X44K Whole Human Genome

DNA microarray slides (cat. G4112F, Agilent) according to the instructions of the manufacturer. An Agilent Technologies Scanner G2505B US45102976 and the Feature Extraction (FE) Software v 9.5.1.1 with the GE2-v5_95_Feb07 Gene Expression protocol were used to scan microarray slides and extract data, respectively.

Preprocessing microarray data

AC1 gene expression data generated at VUmc was preprocessed in an identical way as those previously preprocessed at UMCU¹⁷. This comprised: 1) extraction of the median signal from the raw data files without background correction, and 2) median and loess within-array normalization as implemented in the Limma-package (<http://www.bioconductor.org>). Preprocessed VUmc and UMCU data sets were combined by limiting both to the probes that overlapped (using their Agilent probe identifiers). Finally, comparability of the expression data of both centers was ensured by a) joint between-array normalization (Aquantile as implemented in the Limma-package), and b) removal of possible batch (i.e. center) effects using the Combat-package³². Raw and processed data are publicly available in the gene expression omnibus (GEO) database (GSE85446).

Data from AC2 were not combined to the other datasets, because of a different reference design: Universal Human Reference RNA (cat. 740000, Agilent Technologies, Santa Clara, CA) in AC1 and a pool of cell line RNA in AC2 (CAL 27, ATCC CRL-2095, American Type Culture Collection, Manassas, VA). AC2 data were preprocessed in the same way as data set AC1. Probes with more than 20% missing values were deleted. AC2 consisted of 106 samples, but seven were excluded because of poor quality MA plots. Remaining missing values were imputed with nearest neighbor averaging with R package impute. For the LNM analysis, two additional patients were excluded because information on the LNM was missing. Raw and processed data are registered in the gene expression omnibus (GEO) database (GSE84846), but are not publicly available until July 25th, 2018 or after publication of this manuscript.

Gene selection

Per data set, the predictive significance for LNM and survival was assessed with the global test^{24,25}. Data sets with significant results ($p < 0.05$) were used for gene selection. For prediction of LNM, we obtained significant results for both AC1 and AC2 (AC1, $p=9.3E-06$; AC2, $p=9.9E-03$), hence both were used for gene selection. For prediction of survival, only AC1 showed predictive significance (AC1, $p=7.8E-3$; AC2, $p=0.73$) and was used for further analysis. This difference is likely explained by a shorter follow-up time in AC2 compared to AC1 (AC1, mean overall follow-up time: AC1: 4.7 years (SD=3.2), AC2: 3.0 years (SD=1.5)).

The selection of genes was based on univariable and multivariable analysis with an equal contribution to the final signature (50% of genes from univariable analysis, 50% from multivariable analysis). For the multivariable selection our aim was to come to an optimal set of genes that orthogonally contribute on top of each other (see Supplementary Example R code below). Due to selection from a large number of genes using limited sample series, it is to be expected that some genes will not validate. Also, the platform transition we conducted increases the probability that genes cannot be validated, although this is somewhat counterbalanced by the technical validation. For this reason we planned some redundancy in the selected genes. This is best achieved by selecting those genes that have the highest signal to noise ratio (e.g. low p -value). The total number of selected genes was limited to 60 genes of interest because of the chosen qPCR array card design (60 target genes + 4 housekeeping genes, 3 replicates, and 2 samples / array card). Univariable analysis included t -tests (LNM) and Cox regression (overall survival). For LNM p -values of AC1 and AC2 were combined with Fisher's combined p -value. P -values were adjusted with the Benjamini-Hochberg procedure to control the false discovery rates (FDR)²⁶. Multivariable analysis consisted of lasso logistic regression (LNM) and lasso Cox regression (overall survival), as implemented in package glmnet in R. To stabilize the selection, the lasso

was run repeated N times per analysis (as a leave-one-out cross-validation (LOOCV)). For LNM, the selection frequencies of AC1 and AC2 were added up. We next selected those genes that were used most often in the models. For survival, models were tested with and without addition of pathological stage of disease (pTNM) and age as unpenalized covariate, but the additions did not change the list of selected genes considerably.

To reduce dimensionality and enrich for relevant predicting genes, previously published HNSCC gene signatures were used as input for gene selection. For LNM, we used a previously published LNM predicting gene profile^{15,16} consisting of 732 probes, which was later validated in a multicenter trial¹⁷. For survival, thoroughly validated prognostic gene signatures were missing. Therefore, we combined a set of 9 prognostic gene expression profiles^{10-12,33-37} (1,426 probes) and an in-house discovered prognostic profile of genes for which copy number alterations and gene expression were best correlated (348 probes). This combined survival profile consisted of 1,762 probes. Twenty genes were selected from the combined survival profile (1,762 probes), and 20 genes were selected from analyses that included all probes (37,622 probes in AC1).

Quantitative real-time PCR

A 384-well Taqman Low-Density Array (TLDA) Card was designed with the selected 60 prognostic genes + 4 housekeeping genes (GAPDH, GUSB, RPL4, RPLP0). Each gene expression assay was represented by 3 replicates. The initial design (TLDA.v1) and optimized design (TLDA.v2) after technical validation (see below) are shown in Supplementary Table 2. One µg of mRNA was treated with DNase I, Amplification Grade (cat. 18068015, Invitrogen; Carlsbad, CA) in a 10 µl reaction volume. The DNase-treated mRNA was subsequently used for cDNA synthesis with the High-Capacity RNA-to-cDNA Kit (cat. 4387406, Applied Biosystems; Foster City, CA) in a 24.4 µl reaction volume. The qPCR reaction mix consisted of (1) 20 µl cDNA (819 µg), (2) 190 µl water, and (3) 210 µl 2X TaqMan Gene Expression Master Mix (cat. 4369016, Applied Biosystems). Subsequently, the reaction mix was loaded on the TLDA cards according to the protocol of the supplier. Reaction mixes of 2 samples were loaded per TLDA card. Experiments were performed on an ABI Prism 7900HT Fast Real-Time PCR System (cat. 4329001, Applied Biosystems). Thermal cycling conditions were: 50°C for 2 minutes; 94.5°C for 10 minutes; 40 cycles of denaturation at 97°C for 30 seconds and annealing and extension at 59.7°C for 1 minute. The median result of a triplicate assay was used in downstream analysis.

Gene expression analysis from qPCR data

For each qPCR reaction, the Ct-value was determined as the cycle number at which the fluorescence signal reached a fixed threshold using the SDS RQ Manager Version 1.2.2 (Applied Biosystems). Next, the Ct-values were normalized to the GUSB expression level, which was the most stable housekeeping gene in this dataset. To select the most stable housekeeping gene, we determined the standard deviation of the gene expression within all samples and correlation of the housekeeping gene to the average gene expression of all target genes (Supplementary Table 7). GUSB had both the lowest SD (SD=0.94) and the highest correlation to the average expression of all target genes (r=0.77).

Technical qPCR validation

The 60 selected target genes were technically validated using a subset of 20 cases from AC2 to evaluate the platform transition. Hence, the qPCR data were correlated to the array data of the same samples. These 20 cases were selected to contain a 1:1 ratio of N0/N+ cases and patients that survived/deceased. For these 20 cases, Pearson's correlation coefficients were calculated between microarray and corresponding qPCR data (Supplementary Table 3). Poor correlation was defined as an r of >1 SD below the mean and a p-value >0.1 (because of the small sample size). Logistic and Cox regression analyses were performed to determine the predictive performance of the genes in this cohort.

Histopathology

Formalin-fixed paraffin embedded slides of the surgical specimens were examined by two specialized pathologists (EB + EMS), according to the guidelines of the Royal College of Pathologists UK (<https://www.rcpath.org/resourceLibrary/dataset-for-histopathology-reporting-of-mucosal-malignancies-of-the-oral-cavity.html>). Tumors were staged according to TNM classification of Malignant Tumors, 7th Edition, published in affiliation of the Union for International Cancer Control (UICC)³⁸. The margin status was evaluated and divided into three groups: (1) involved margins when carcinoma was present in or within 1 mm of the margin, (2) negative margins when the excised carcinoma was > 5 mm from the surgical margin, and (3) close margins when the tumor was 1-5 mm from the surgical margin³⁹. For model building, the margin status was subsequently subdivided in two groups: involved margins when carcinoma was present in or within 1 mm of the margin (R+); or negative margins, when the excised carcinoma was > 1 mm from the surgical margin (R0). The presence of lymph node metastasis (LNM) was determined by standard histopathological examination of the neck dissection specimen if present. When the neck was left untreated, two scenarios were possible: a patient was diagnosed N+ when a delayed lymph node metastasis developed during follow-up (\leq three years after treatment) or remained N0 when not. In the different cohorts, 128 of 150 (85.3%, AC1), 89 of 99 (89.9%, AC2) and 103 of 125 (82.4%, qPCR cohort) the neck was treated with a primary neck dissection. Extracapsular spread (ECS) was present if the tumor extended beyond the capsule of the lymph node. When there was doubt, the case was classified as having ECS according to the guidelines of the Royal College of Pathologists UK⁴⁰. We created a pathological composite variable (pCompVar) that was scored positive if ECS or R+ or >1 LNM was present.

Clinical data

Several clinical variables were used for prognostic model building. These included age at diagnosis, gender, smoking behavior in packyears (1 packyear equals 20 cigarettes a day during 1 year), ECOG Performance Status⁴¹, and comorbidity. Comorbidity was classified using the Adult Comorbidity Evaluation 27 (ACE-27)⁴², in which an overall comorbid score is graded in four levels: none, mild, moderate or severe. For smoking we only considered the packyears in the model building. Compared to categorical smoking variables, packyears contains the most information about the smoking habits and was also the most significant smoking variable for OS.

Outcomes

Overall survival (OS) was defined as time from date of incidence to death from any cause. Disease free survival (DFS) was defined as time from date of incidence to development of locoregional recurrence, distant metastasis or second primary HNSCC. Mean survival times for the various data sets were calculated with the reverse Kaplan-Meier as suggested by Schemper et al.⁴³ Patients who died of other causes or develop second primary tumors outside the head and neck region (SPT), were censored on the date of death or incidence date of the SPT. Local recurrences were scored when these developed within two centimeters of the index tumor and within three years after therapy, whereas a regional recurrence was documented when it developed in a treated neck within three years after treatment.

Statistical analysis of the RT-qPCR dataset

For the qPCR data, the univariable association of delta Ct values of the selected genes with either LNM or OS/DFS was determined with logistic or Cox regression, respectively. Multivariable models with the selected genes were made with logistic ridge regression (LNM) or Cox ridge regression (OS/DFS). For the clinical variables univariable p-values of clinical variables were determined by Cox proportional hazards regression (OS, DFS)

or logistic regression (LNM). Patients with moderate and severe comorbidity (ACE-27) were considered as one group in the analysis, because the group with severe comorbidity (ACE-27) was very small. TNM-stage was dichotomized as early stage disease (pTNM I+II) and advanced stage disease (pTNM III+IV). Variables with p-value lower than 0.15 were considered as candidates for a multivariable model. For LNM prediction, no clinical variables met this criterion. Next, stepwise regression was performed to identify a multivariable model with clinical variables (using procedure 'step' in R). Stepwise selection with Akaike Information Criterion (AIC) was performed and in each step a variable was added or dropped, which identified the best model. For OS, the stepwise selection procedure selects age and packyears. The prediction models for outcome consisted of (1) prognostic genes only, (2) clinical variables and pathological TNM-stage (pTNM), (3) clinical variables and a composite pathological variable (positive if ECS or R+ or >1 LNM was present), and the combinations (4) 1+2 and (5) 1+3. In combined clinical and genomic models, the clinical variables were not penalized and the genes were incorporated with a ridge penalty to avoid overfitting. The predictive performance was measured by area-under-the-ROC-curve (AUC) and integrated AUC (iAUC)⁴⁴ at 5-year follow-up time for LNM and OS/DFS, respectively, complemented for LNM by the NPV, i.e. the proportion of true negatives among all negative tests. Model performance was assessed by bootstrapping, confidence intervals around the AUC, sensitivity, specificity, PPV, and NPV were calculated according to methods described by Jiang et al.⁴⁵⁻⁴⁷ (see Supplementary Outline of Statistics and Supplementary Example R code). Model performance only takes into account the uncertainty in the genomic, clinical, and pathological coefficients. The variable selection of clinical variables was not bootstrapped, the pathological variables (pTNM and CompVar) were selected based on their known clinical relevance. For the genomics variables we did not perform further selection on the RT-qPCR data. For OS and RFS the subgroup analysis was performed by refitting the model to the cases of that subgroup. For LNM subgroup analysis, refitting was not possible due to the small sample size of the subgroup (n=54) with a low number of cases (15). Therefore, the AUC for the subgroup was computed by first fitting the model to all cases (n=125), and then considering the subgroup. Additive value of the gene signature was assessed with the global test^{24,25}. All statistical tests performed were two-sided. In multiple testing settings, univariable p-values were corrected using the Benjamini-Hochberg FDR procedure²⁶.

External validation with TCGA RNAseq dataset

Only the 279 patients that were included in the Cancer Genome Atlas Network publication¹⁹ were used for this analysis, because the RNAseq derived HPV-status, which was considered the most accurate, was not available for the other cases. Of these cases, the normalised RNASeqv2 TCGA data were downloaded with R package TCGA2STAT. Additional clinical information was downloaded directly from the Broad Institute (http://gdac.broadinstitute.org/runs/awg_hnsc__2013_03_30/reports/cancer/HNSC-TP-HPV-positive-36/mutsignozzlereportscv/nozzle.html). Only HPV-negative tumors of the oral cavity were considered (n=160). For lymph node metastasis, patients with a pathological NX-stage were excluded. This left 133 patients for lymph node metastases (LNM). For OS, the survival time of one patient was missing and 159 patients were available for analysis. The LNM outcome was defined as having a pathological N-stage larger than 0. Of the 60 genes selected on the microarray data, 1 gene could not be matched to the TCGA data (LRCOL1).

Before analysis the data were transformed by taking the square root and scaling the data (e.g. all genes transformed to zero mean and unit variance). For OS and for LNM, the global test was used to assess the association with the genomic signatures. Further predictive performance was assessed by fitting and bootstrapping a logistic (for LNM) and Cox (for OS) regression model with ridge penalization.

Sample size considerations

Exact sample size calculations are inherently difficult for ridge regression. They also require knowledge of the effect sizes, which are unknown in our multivariate setting. To provide some insights regarding correct

sample size, we performed some ad hoc tests with the qPCR cohort. Random samples of 45-115 patients were repeatedly drawn (50 times) without replacement from the data, supplemented with the actual data for $n=125$. For each outcome variable, the global test was used to assess the predictive performance of the genomic signatures. For each same sample size we took the medium p-value across the random samples. Sample sizes of 85 cases and more gave consistent p-values <0.05 for each outcome variable (see Supplementary Figure 6), assuring that the sample size of 125 is sufficient to assess the performance of the signatures.

Relation of the genomic signatures to other prognostic markers

We additionally analyzed the association between the prognostic markers and the OSsig (here taken as the linear predictor of the Cox ridge regression, i.e. the log of the hazard ratios), as recommended in REMARK criterion 14 (Supplementary Table 6). In this analysis we considered the variables used in the prognostic models (i.e. age, smoking, pTNM, pCompVar) and additionally considered gender and comorbidity (ACE27). For the age and packyears, a Pearson's correlation coefficient and an additional p-value were calculated. For sex, pTNM, and pCompVar we performed a t-test and for ACE27 we performed an ANOVA. Significant correlation between OSsig and gender, smoking, ACE27 and pCompVar were found (Supplementary Figure 7). However, as can be seen in this figure, the size of the effects was small. Secondly, we assessed the iAUC of the genomic predictor in different subgroups (Supplementary Table 8). Subgroups included were: (1) pCompVar negative and positive; (2) Age <70 and ≥ 70 years at diagnosis; (3) Smoking: packyears $<$ median and \geq median value in this dataset; (4) Comorbidity (ACE27): ACE27 0-1 and ACE27 2-3; (5) Male and female gender; and (6) pathological stage I+II and III+IV. This analysis showed that the OSsig has good discriminative power in the various subgroups.

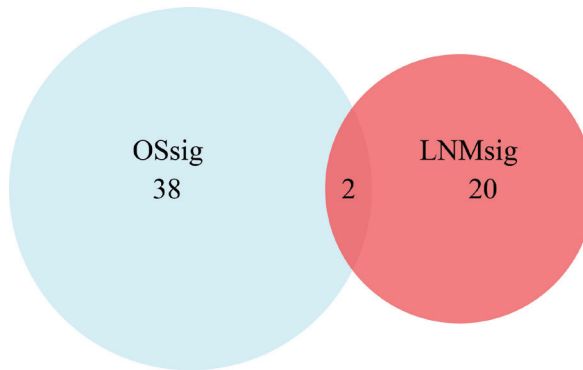
SUPPLEMENTARY OUTLINE OF STATISTICS

1. Gene selection with microarray data.
 - a. Univariable selection
 - i. p-value per gene with false discovery rate (FDR) control.
 1. Welch t-test for LNM
 2. Cox regression for OS
 - b. Multivariable selection with lasso (see example code)
 - i. Repeatedly fitting the lasso. Genes are ranked based on their selection frequency across the lasso fits (see example code of the lasso selection).
 - ii. Analysis conducted with and without mandatory covariates. Mandatory covariates were not subject to the lasso penalty (e.g. unpenalized).
 - iii. Logistic regression for LNM, Cox regression for OS
2. Technical validation
 - a. Pearson's correlation coefficient (and associated p-value) between qPCR – microarray data per gene.
3. Validate selected genes on independent data (i.e. qPCR data).
 - a. Univariable assessment
 - i. p-value per gene with false discovery correction (FDR) control.
 1. Logistic regression for LNM
 2. Cox regression for OS/RFS
4. Fit with selected genes on the (independent) qPCR data.
 - a. Low dimensional models (i.e. clinical and/or pathological) fitted with standard regression techniques.
 - i. Clinical variable are selected on the qPCR data for OS. First we conducted a univariate screening with p-value of 0.15. Next the clinical model was made by stepwise regression based on AIC.
 - b. Genomics models fitted with ridge regression
 - c. Combined models (e.g. clinical, and/or pathological and/or genomics) for RFS/OS fitted with ridge regression. Clinical and/or pathological are not subject to the ridge penalty.
5. Predictive accuracy of the models is assessed by bootstrapping.
 - a. Bootstrap assessed the parameter uncertainty.
 - b. For the clinical data the variable selection process was not bootstrapped.
 - c. For genomics and pathological variables there was no further variable selection.
 - d. For bootstrap code see <http://github.com/DennisBeest/BootPredError>.
6. Step 4b and step 5 are repeated with the (independent) TCGA data.

SUPPLEMENTARY EXAMPLE R CODE OF THE MULTIVARIABLE GENE SELECTION (LASSO)

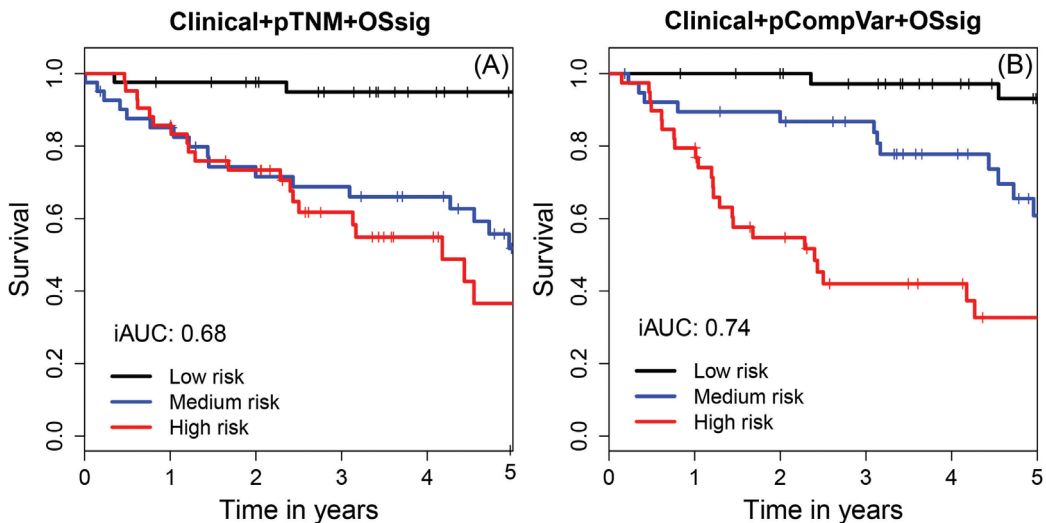
```
#####
#---Example code
library(glmnet)
#####
#---Simulated some survival data, replace these by real data
#####
P <- 200
N <- 100
Train <- matrix(nrow=N,ncol=P)
Train[] <- runif(P*N)
Survival <- rep(c(0,1),each=N/2)
Train[Survival==1,1:5] <- Train[Survival==1,5]+0.5
Time <- runif(N)
Time[Survival==1] <- Time[Survival==1]/2
colnames(Train) <- 1:P
penfac <- rep(1,times=P)
#####
#---Selection with lasso in the form of a LOOCV.
#---Alternatively the lasso can be run repeatedly on the whole data, or on bootstraps.
#---The lasso is likely to select a different set of variables each time it is run on slightly different data or when
the cross-validation folds are changed. Especially when the the data are stongly correlated. The aim of running
it repeatedly is to stabilise the selection.
#---An unpenalized covariate can be incorporated by setting penfac to 0 for that variable.
#####
N <- length(Survival)      #Number of patients
Selected <- list()         #List for saving selected genes
SavePrediction <- numeric() #Optionally for saving cross-validated predictions
for(i in 1:N)              #Repeat for each patient
{
  #####
  #Leave one patient out
  Y <- cbind(time=Time[-i],status=Survival[-i])
  X <- Train[-i,]
  #####
  #Fit lasso
  model <- cv.glmnet(X,Y,family="cox",standardize = FALSE,alpha = 1,nfolds=5,penalty.factor=penfac)
```

```
#####
#Keep track of selected variables
betas <- model$glmnet.fit$beta[,model$glmnet.fit$lambda==model$lambda.min]
Selected[[i]] <- names(betas)[which(betas!=0)]
#####
#Optionally get an indication of the predictive value
XTest <- Train[i,,drop=FALSE]
SavePrediction[i] <- predict(model,newx=XTest,s=c("lambda.min"))
}
#####
#----Add selected variables together and sort/rank
tab <- table(unlist(Selected))
o <- order(tab,decreasing=TRUE)
print(cbind(tab[o]))
#####
#----End of code
```

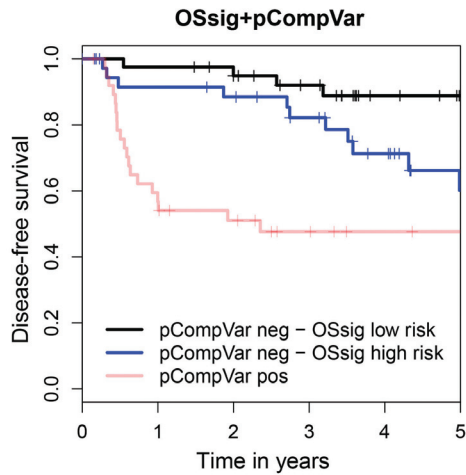
3

Supplementary Figure 1. Venn diagram of selected gene signatures shows 2 overlapping genes between OSsig and LNMsig. Venn diagram of selected overall survival gene signature (OSsig, 40 genes) and lymph node metastasis gene signature (LNMsig, 22 genes) shows that 2 genes overlap, limiting the combined signatures to 60 genes. LNMsig, lymph node metastasis signature; OSsig, overall survival signature.



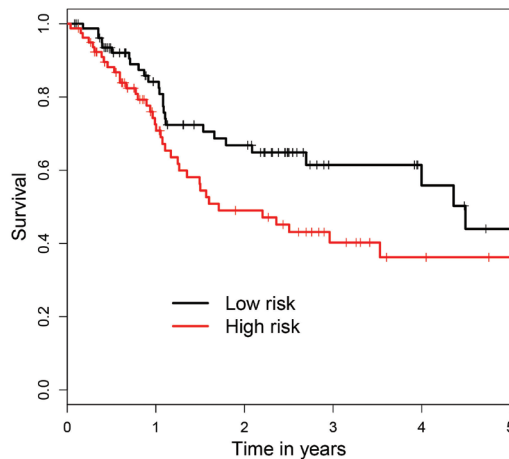
Supplementary Figure 2. Best predicting integrated models of clinical variables, histopathological variables and the overall survival signature (OSsig).

(A-B) Results of the Kaplan-Meier analysis are depicted for overall survival in the independent validation cohort using the best predicting models with risk groups defined by tertile predicted hazards of (A) the OSsig combined with significant clinical variables (i.e. age at diagnosis, smoking) and pathological TNM stage (pTNM) (iAUC=0.68, OSsig: $P=0.03$ (global test)), and (B) the OSsig combined with the same clinical variables and the a composite histopathology variable (pCompVar) that was scored positive if extracapsular spread (ECS) or involved resection margins (R+) or >1 lymph node metastasis was present; all three variables are currently used as indicators for adjuvant treatment (iAUC=0.74, OSsig: $P=0.02$ (global test)). Area under the curve was integrated over 5 year follow-up time. Tick marks on curves indicate censoring. iAUC, integrated Area Under the Curve; OSsig, overall survival signature; pCompVar, pathological composite variable; pTNM, pathological TNM stage.



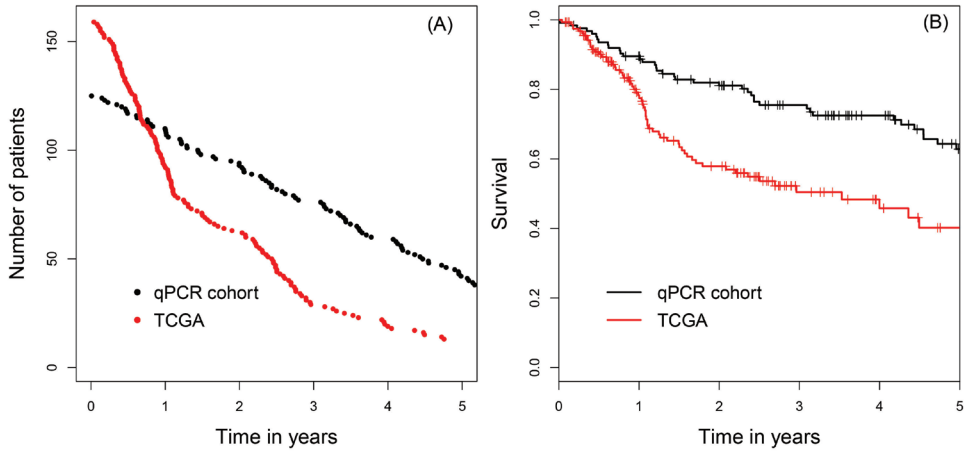
Supplementary Figure 3. The Overall Survival genomic signature (OSSig) predicted disease-free survival of oral squamous cell carcinoma (OSCC) in a subgroup of prognostically favorable patients.

A subgroup of 79 prognostically favorable patients was identified based on histopathological variables, i.e. tumor-free margins (R0), ≤ 1 lymph node metastasis (LNM), and without extracapsular spread (ECS-neg). Depicted is a Kaplan-Meier analysis for disease-free survival in these pCompVar-negative patients of the independent validation group with risk groups defined by median predicted hazards of the OSSig (black and blue lines; integrated area under the curve (iAUC)=0.65, OSSig: $P=7E-3$ (global test)). Area under the curve was integrated over 5 year follow-up time. Abbreviations: iAUC, integrated Area Under the Curve; OSSig, Overall Survival signature; pCompVar, pathological composite variable.



Supplementary Figure 4. Additional external validation of the overall survival signature (OSSig).

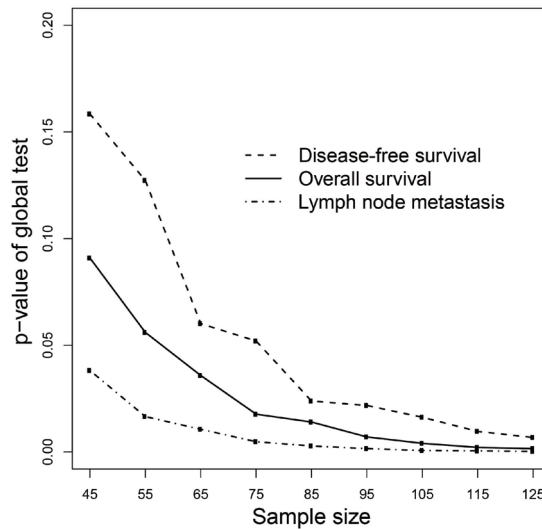
Kaplan-Meier analysis of overall survival with risk groups defined by median predicted hazards by the OSSig. RNAseq data of the TCGA cohort head and neck squamous cell carcinoma cohort were used of HPV-negative, OSCC patients ($n=159$; iAUC=0.59; OSSig: $P=0.02$ (global test)). Area under the curve was integrated over 5 year follow-up time. Tick marks on curves indicate censoring. Abbreviations: iAUC, integrated Area Under the Curve; OSSig, Overall Survival signature.



3

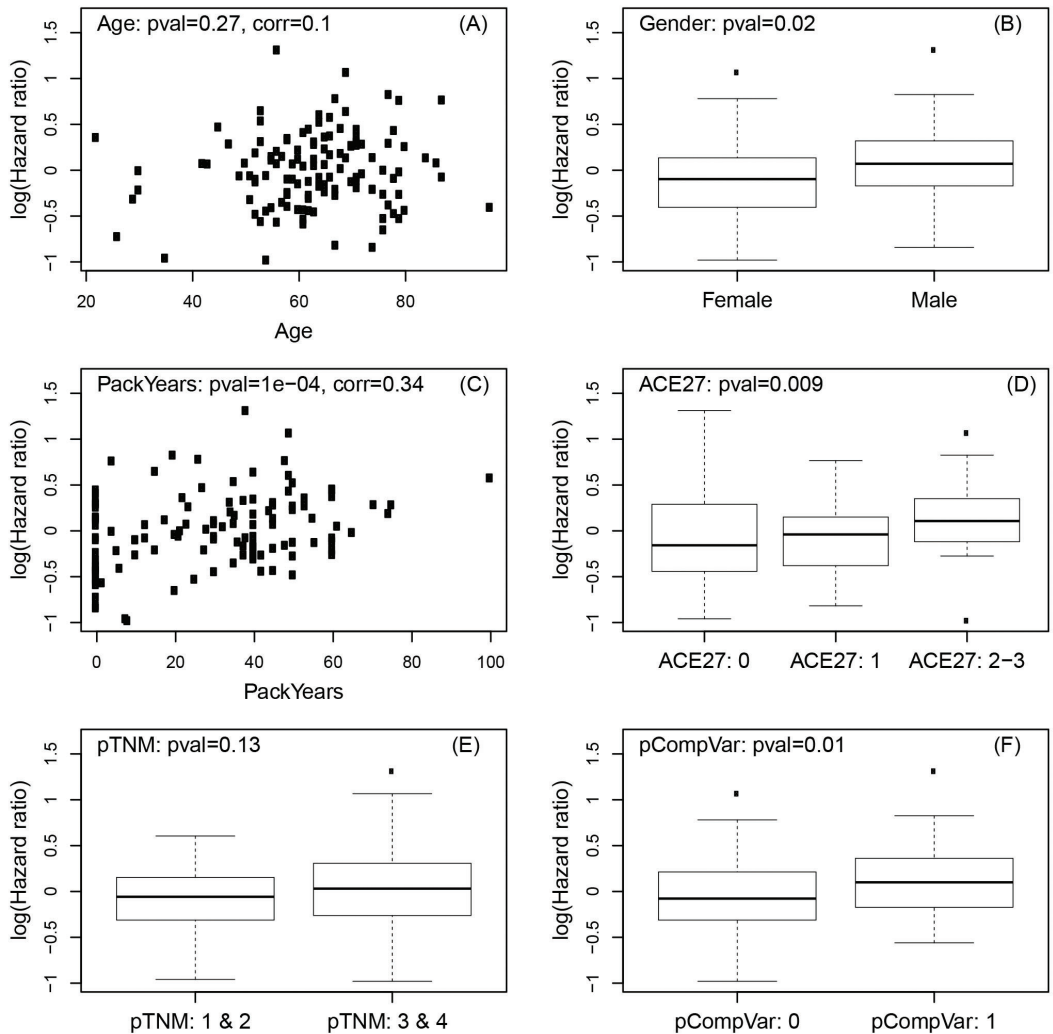
Supplementary Figure 5. Comparison of follow-up time and baseline survival curves shows significant differences between our qPCR validation cohort and the TCGA cohort.

(A) Number of patients under consideration (y-axis) in relation to follow-up time (x-axis) of qPCR cohort (black) and TCGA cohort (red). (B) Baseline Kaplan-Meier analysis of qPCR cohort (black) and TCGA cohort (red) differed significantly (cox regression: HR= 2.0, 95% CI =1.4–2.9), $P=3E-4$).



Supplementary Figure 6. Random sampling from independent qPCR cohort shows clear relationship between sample size and global test p-value, and provides rationale for the tested sample size.

Random samples of increasing sample size were repeatedly (50 times) drawn without replacement from the data (y-axis). For each outcome variable, the global test was used to assess the predictive performance of the genomic signatures. P-values were averaged between random samples of the same size (x-axis). Sample sizes of 85 cases and more gave consistent p-values <0.05 for each outcome variable, assuring that the sample size of 125 cases of the independent validation cohort should be sufficient to assess the performance of the signatures.



Supplementary Figure 7. Relation of Overall Survival signature (OSSig) to other prognostic markers.

(A-F) Relation of the OSSig linear predictor of the Cox ridge regression, i.e. the log of the hazard ratios (y-axis), and other prognostic variables (x-axis). A Pearson's correlation coefficient and an additional p-value were calculated for numerical variables, for ACE27 we performed an ANOVA, and for the remaining categorical variables, a t-test was performed. Relation between OSSig and (A) age (in years, $r=0.1$, $P=0.27$), (B) gender ($P=0.02$), (C) smoking (in packyears; $r=0.34$, $P=0.0001$), (D) comorbidity (ACE27; $P=0.009$), (E) pathological TNM stage (pTNM; $P=0.13$), and (F) a composite pathology variable (pCompVar) that was positive if extracapsular spread or tumor-positive resection margins or >1 lymph node metastasis was present ($P=0.01$). For each marker the size of the effects was small, even when a significant relation was found. corr, Pearson's correlation coefficient; pCompVar, pathological composite variable; pTNM, pathological TNM stage.

Supplementary Table 1. Genes with false discovery rate <0.1 on microarray data

FDR < 0.10 for survival of AC1					FDR based on Fisher combined p-value < 0.10 for N stage of AC1 + AC2					
Gene	Probe	FDR survival	p-value Survival	p-value Recurrence	Gene	Probe	Fisher's combined test FDR	Fisher's combined test p-value	p-value AC1	p-value AC2
TANC2	A_23_P431404	5.76E-03	1.53E-07	5.97E-02	FN1	A_24_P334130	2.53E-09	2.50E-06	8.3E-08	1.3E-03
SELP	A_23_P137697	2.55E-02	1.69E-06	2.65E-02	P4HA1	A_24_P406693	5.20E-08	2.57E-05	4.0E-05	6.3E-05
C9orf116	A_23_P422115	2.55E-02	2.06E-06	4.13E-02	ADAM12	A_23_P350512	1.03E-07	3.39E-05	8.4E-08	6.1E-02
C9orf50	A_23_P406785	2.55E-02	2.71E-06	1.40E-01	FN1	A_24_P85539	5.35E-07	1.32E-04	3.5E-06	8.4E-03
CDK9	A_23_P158083	2.89E-02	4.99E-06	5.30E-03	SCG5	A_23_P62081	1.03E-06	2.04E-04	2.4E-07	2.4E-01
ENST00000362067	A_24_P919789	2.89E-02	6.13E-06	5.54E-03	SPOCK1	A_24_P354689	1.40E-06	2.31E-04	4.8E-06	1.7E-02
FLJ25410	A_23_P89101	2.89E-02	6.08E-06	2.12E-01	TIMM8B	A_23_P98382	1.64E-06	2.31E-04	3.4E-04	2.8E-04
SPINK4	A_23_P71880	2.89E-02	4.37E-06	4.20E-01	AL050204	A_24_P937691	3.06E-06	3.77E-04	5.0E-04	3.7E-04
R78584	A_24_P225862	3.41E-02	9.05E-06	7.70E-03	COL5A1	A_23_P158593	3.96E-06	4.35E-04	1.2E-06	2.1E-01
ZNF366	A_23_P407096	3.41E-02	9.50E-06	3.93E-02	ADAM12	A_23_P202327	6.02E-06	5.95E-04	3.0E-06	1.3E-01
TCEB3C	A_23_P315910	3.41E-02	9.96E-06	1.76E-01	COL5A1	A_23_P83818	1.28E-05	1.15E-03	5.8E-06	1.5E-01
CCDC88	A_23_P24384	4.39E-02	1.40E-05	2.16E-03	COL6A1	A_24_P331918	1.54E-05	1.18E-03	2.2E-05	4.8E-02
ADCY4	A_23_P381261	5.13E-02	3.01E-05	1.02E-03	SERPINH1	A_23_P76006	1.55E-05	1.18E-03	6.9E-05	1.5E-02
LOC642730	A_24_P683013	5.13E-02	2.59E-05	3.38E-03	EVA1	A_23_P150379	1.71E-05	1.21E-03	3.8E-05	3.1E-02
BC015370	A_24_P205154	5.13E-02	3.56E-05	3.76E-03	MGC11257	A_23_P134477	2.22E-05	1.46E-03	1.4E-03	1.1E-03
CCDC88	A_23_P24389	5.13E-02	2.92E-05	5.84E-03	SDC2	A_24_P380734	2.61E-05	1.61E-03	4.3E-04	4.3E-03
RASA4	A_24_P943263	5.13E-02	3.31E-05	1.17E-02	CALD1	A_23_P42575	3.18E-05	1.85E-03	1.1E-05	2.1E-01
C21orf125	A_32_P214178	5.13E-02	2.47E-05	1.20E-02	COL11A1	A_23_P11806	3.53E-05	1.87E-03	8.3E-05	3.1E-02
ENST00000380632	A_32_P6646	5.13E-02	3.36E-05	1.42E-02	LGALS1	A_23_P166459	3.59E-05	1.87E-03	1.9E-05	1.4E-01
CBFA2T3	A_23_P500741	5.13E-02	2.89E-05	3.34E-02	FAP	A_23_P56746	4.97E-05	2.46E-03	1.6E-05	2.3E-01
IL27RA	A_24_P348326	5.13E-02	3.41E-05	4.92E-02	MLL	A_24_P281913	5.54E-05	2.61E-03	4.4E-05	9.4E-02
NRIP3	A_23_P47682	5.13E-02	2.54E-05	7.10E-02	PLA2G4B	A_23_P403424	6.41E-05	2.88E-03	2.6E-04	1.9E-02
TMEM31	A_23_P352717	5.13E-02	2.99E-05	1.09E-01	CSTB	A_23_P154894	6.80E-05	2.92E-03	4.5E-04	1.2E-02
PTPN14	A_23_P149111	5.13E-02	3.68E-05	1.63E-01	CCND1	A_24_P193011	7.71E-05	3.18E-03	1.2E-03	5.0E-03
SPATA17	A_23_P346912	5.13E-02	3.18E-05	2.06E-01	COL5A2	A_23_P10391	8.54E-05	3.38E-03	2.2E-05	3.0E-01
CCND1	A_24_P193011	5.13E-02	2.43E-05	2.54E-01	TRIO	A_24_P42603	9.49E-05	3.61E-03	7.5E-05	9.9E-02
ESM1	A_23_P144843	5.13E-02	2.67E-05	7.80E-01	POSTN	A_24_P347411	9.94E-05	3.64E-03	2.0E-04	3.9E-02
RASGRP2	A_23_P64058	5.18E-02	3.85E-05	2.70E-01	LARP6	A_23_P117782	1.09E-04	3.83E-03	1.5E-04	5.8E-02
ZNF406	A_32_P109922	5.21E-02	4.01E-05	2.72E-01	KDELRL2	A_24_P42517	1.15E-04	3.87E-03	1.3E-04	7.1E-02
LOC645277	A_32_P49867	5.66E-02	5.56E-05	6.30E-03	SEC11L1	A_23_P380917	1.20E-04	3.87E-03	2.6E-05	3.7E-01
PVRL3	A_23_P80763	5.66E-02	5.51E-05	7.92E-03	TPM2	A_23_P216501	1.21E-04	3.87E-03	6.6E-05	1.5E-01
C6orf189	A_23_P145054	5.66E-02	4.84E-05	2.59E-02	IGF1R	A_23_P305680	1.32E-04	4.01E-03	2.7E-03	3.9E-03
LOC645733	A_32_P3572	5.66E-02	5.25E-05	3.86E-02	CLEC11A	A_23_P153489	1.34E-04	4.01E-03	2.3E-04	4.7E-02
LOC92689	A_23_P132915	5.66E-02	5.49E-05	1.06E-01	DENND2D	A_23_P85952	1.56E-04	4.54E-03	1.2E-03	1.1E-02
THC2278340	A_24_P479364	5.66E-02	4.78E-05	2.16E-01	TGM3	A_23_P57118	1.63E-04	4.60E-03	1.9E-03	6.8E-03
TMEFF1	A_24_P274987	5.66E-02	5.54E-05	2.44E-01	TPM1	A_23_P391586	1.77E-04	4.80E-03	6.2E-05	2.4E-01

Supplementary Table 1. (continued)

FDR < 0.10 for survival of AC1					FDR based on Fisher combined p-value < 0.10 for N stage of AC1 + AC2					
Gene	Probe	FDR survival	p-value Survival	p-value Recurrence	Gene	Probe	Fisher's combined test FDR	Fisher's combined test p-value	p-value AC1	p-value AC2
RESP18	A_24_P59236	5.66E-02	4.68E-05	4.42E-01	PPL	A_23_P106906	1.80E-04	4.80E-03	8.1E-04	1.8E-02
CPNE5	A_23_P360804	5.78E-02	5.83E-05	1.57E-02	TPM1	A_32_P89709	1.89E-04	4.89E-03	9.5E-05	1.6E-01
TNFRSF10B	A_23_P169030	5.84E-02	6.51E-05	1.26E-01	TPM1	A_23_P206018	1.96E-04	4.89E-03	1.2E-04	1.4E-01
RAI1	A_23_P77807	5.84E-02	6.21E-05	1.37E-01	FBXO32	A_23_P82814	2.00E-04	4.89E-03	3.5E-03	4.8E-03
OPRK1	A_32_P33576	5.84E-02	6.39E-05	2.52E-01	CCND1	A_24_P124550	2.03E-04	4.89E-03	1.0E-03	1.6E-02
EFNA1	A_23_P113005	5.84E-02	6.10E-05	4.14E-01	C1QTNF6	A_24_P211565	2.12E-04	4.89E-03	4.9E-05	3.6E-01
SESTD1	A_23_P367610	5.86E-02	6.81E-05	4.26E-02	NDUFV3	A_23_P211285	2.20E-04	4.89E-03	3.1E-03	6.0E-03
FLT3	A_23_P99442	5.86E-02	6.85E-05	1.79E-01	COL1A2	A_24_P265274	2.21E-04	4.89E-03	2.1E-04	8.9E-02
GCET2	A_24_P182947	6.03E-02	7.21E-05	1.22E-01	SPARC	A_23_P7642	2.23E-04	4.89E-03	6.3E-05	3.0E-01
AK097371	A_24_P661612	6.21E-02	8.62E-05	4.76E-04	NID2	A_23_P163087	2.28E-04	4.90E-03	2.5E-05	7.8E-01
NARG2	A_32_P129419	6.21E-02	9.78E-05	1.08E-02	SRPX2	A_23_P136978	2.33E-04	4.90E-03	2.1E-04	9.2E-02
FBXO36	A_23_P432554	6.21E-02	9.64E-05	6.28E-02	ALOX12B	A_23_P83634	2.60E-04	5.35E-03	6.8E-04	3.2E-02
RP11-138L21.1	A_23_P20532	6.21E-02	8.32E-05	6.56E-02	RAB3D	A_24_P236956	2.85E-04	5.74E-03	1.1E-03	2.3E-02
WDR31	A_24_P6674	6.21E-02	8.11E-05	7.44E-02	TGM1	A_23_P65618	2.91E-04	5.75E-03	6.1E-03	4.1E-03
IL18	A_23_P104798	6.21E-02	9.75E-05	1.43E-01	AK022065	A_24_P478423	3.02E-04	5.86E-03	4.7E-03	5.5E-03
COL4A5	A_24_P290153	6.21E-02	8.43E-05	1.69E-01	RAB10	A_23_P165879	3.26E-04	6.20E-03	5.4E-02	5.3E-04
STC2	A_23_P110686	6.21E-02	9.89E-05	1.78E-01	SERPINB2	A_24_P245379	3.73E-04	6.96E-03	7.4E-04	4.4E-02
BANK1	A_23_P10232	6.21E-02	9.29E-05	1.88E-01	DBI	A_23_P79199	3.87E-04	7.08E-03	3.0E-02	1.2E-03
NAPSA	A_23_P90130	6.21E-02	9.36E-05	2.05E-01	TRIM29	A_23_P203267	4.16E-04	7.47E-03	6.0E-04	6.2E-02
P2RY14	A_24_P165864	6.21E-02	8.48E-05	3.05E-01	CALD1	A_24_P921366	4.28E-04	7.55E-03	4.3E-05	9.0E-01
CTTN	A_23_P202823	6.21E-02	8.44E-05	3.06E-01	P4HA2	A_23_P30363	4.50E-04	7.80E-03	7.2E-05	5.6E-01
TNFRSF19	A_24_P56310	6.21E-02	8.20E-05	3.75E-01	RGS5	A_23_P46045	4.62E-04	7.81E-03	4.7E-03	8.9E-03
CXCL13	A_23_P121695	6.21E-02	9.00E-05	5.54E-01	MLL	A_24_P127812	4.66E-04	7.81E-03	3.2E-04	1.3E-01
GLCE	A_23_P151870	6.21E-02	8.78E-05	6.54E-01	MGC4677	A_24_P273143	5.07E-04	8.34E-03	2.6E-04	1.8E-01
FBXO36	A_24_P254702	6.69E-02	1.08E-04	1.51E-01	RAB11FIP1	A_23_P31873	5.28E-04	8.56E-03	2.8E-04	1.8E-01
FBXO9	A_23_P254120	6.74E-02	1.31E-04	7.98E-03	P4HA2	A_23_P18966	6.04E-04	9.54E-03	1.5E-04	3.6E-01
SELE	A_23_P97112	6.74E-02	1.34E-04	1.45E-02	HSPC159	A_23_P430818	6.08E-04	9.54E-03	4.6E-03	1.2E-02
CCDC48	A_23_P166566	6.74E-02	1.29E-04	1.89E-02	COL5A2	A_23_P33196	6.23E-04	9.61E-03	6.4E-05	9.0E-01
CCDC113	A_24_P73730	6.74E-02	1.34E-04	3.53E-02	INVS	A_23_P157970	6.32E-04	9.61E-03	8.7E-05	6.8E-01
AFF1	A_23_P169619	6.74E-02	1.27E-04	4.44E-02	TGFB1	A_23_P156327	6.79E-04	1.01E-02	1.0E-04	6.1E-01
GFRA2	A_24_P96505	6.74E-02	1.29E-04	6.18E-02	COL5A3	A_23_P55749	6.83E-04	1.01E-02	2.6E-04	2.5E-01
CLEC3B	A_23_P69497	6.74E-02	1.33E-04	8.92E-02	UBTD1	A_23_P161501	6.98E-04	1.01E-02	5.2E-04	1.3E-01
MTL5	A_24_P25234	6.74E-02	1.32E-04	9.66E-02	EIF4A2	A_32_P134402	7.09E-04	1.01E-02	2.3E-01	2.9E-04
KIAA0746	A_23_P426021	6.74E-02	1.34E-04	1.15E-01	TAGLN	A_23_P87013	7.13E-04	1.01E-02	7.3E-03	9.2E-03
PPP1R16B	A_23_P352535	6.74E-02	1.24E-04	1.28E-01	GDPD3	A_23_P26511	8.32E-04	1.16E-02	5.2E-03	1.5E-02
CD19	A_23_P113572	6.74E-02	1.33E-04	2.01E-01	COL6A1	A_32_P32254	8.43E-04	1.16E-02	1.7E-04	4.7E-01

Supplementary Table 1. (continued)

FDR < 0.10 for survival of AC1					FDR based on Fisher combined p-value < 0.10 for N stage of AC1 + AC2					
Gene	Probe	FDR survival	p-value Survival	p-value Recurrence	Gene	Probe	Fisher's combined test FDR	Fisher's combined test p-value	p-value AC1	p-value AC2
THC2375612	A_32_P144999	6.74E-02	1.26E-04	2.29E-01	SEC11L1	A_24_P79413	8.68E-04	1.17E-02	1.5E-04	5.5E-01
BTN3A2	A_24_P252078	6.74E-02	1.16E-04	5.02E-01	DEFB103A	A_23_P169017	8.84E-04	1.18E-02	1.6E-02	5.3E-03
BTN3A2	A_23_P391264	6.74E-02	1.30E-04	5.16E-01	SNRP70	A_23_P4902	9.38E-04	1.24E-02	2.3E-03	4.0E-02
LOC149351	A_24_P520767	7.05E-02	1.42E-04	1.77E-02	GALNT2	A_24_P353794	9.96E-04	1.29E-02	1.7E-03	5.7E-02
AK000901	A_32_P126410	7.35E-02	1.50E-04	4.16E-01	SPINK5	A_23_P356494	1.01E-03	1.29E-02	1.1E-02	9.1E-03
C14orf81	A_24_P153558	7.43E-02	1.56E-04	2.52E-02	OPN3	A_23_P74391	1.15E-03	1.41E-02	2.1E-03	5.5E-02
THC2319172	A_32_P875465	7.43E-02	1.54E-04	5.18E-01	CDH2	A_23_P38732	1.15E-03	1.41E-02	1.8E-04	6.5E-01
C12orf35	A_24_P273561	7.56E-02	1.66E-04	7.35E-02	PRSS23	A_23_P150789	1.19E-03	1.41E-02	3.1E-04	3.9E-01
IL3RA	A_32_P217750	7.56E-02	1.67E-04	1.23E-01	COL6A3	A_32_P156322	1.20E-03	1.41E-02	2.9E-03	4.1E-02
BLNK	A_24_P64344	7.56E-02	1.68E-04	1.69E-01	EVA1	A_24_P278552	1.20E-03	1.41E-02	5.5E-03	2.2E-02
MS4A1	A_23_P116371	7.56E-02	1.66E-04	2.37E-01	IGHG1	A_23_P158817	1.20E-03	1.41E-02	1.5E-03	8.0E-02
FCRL3	A_23_P103803	7.56E-02	1.69E-04	2.56E-01	PLA2G4B	A_23_P218203	1.20E-03	1.41E-02	8.4E-04	1.4E-01
TCL1A	A_23_P357717	7.57E-02	1.71E-04	3.35E-01	SLC2A4RG	A_23_P102575	1.26E-03	1.47E-02	2.3E-03	5.6E-02
THC2444078	A_23_P88988	7.69E-02	1.76E-04	7.49E-02	MAN1B1	A_23_P94857	1.35E-03	1.55E-02	2.2E-04	6.1E-01
STEAP3	A_24_P200000	7.98E-02	1.91E-04	6.49E-03	COL5A2	A_32_P218734	1.37E-03	1.55E-02	1.4E-03	9.8E-02
CCDC93	A_23_P91062	7.98E-02	1.88E-04	1.60E-01	IGHG1	A_23_P218126	1.42E-03	1.60E-02	1.1E-03	1.3E-01
C6orf32	A_24_P941359	7.98E-02	1.86E-04	7.19E-01	ADC	A_23_P103371	1.45E-03	1.61E-02	1.8E-03	8.1E-02
ERGIC1	A_23_P333227	7.98E-02	1.90E-04	7.63E-01	WAC	A_23_P201996	1.54E-03	1.69E-02	2.5E-03	6.2E-02
AY358804	A_23_P76136	8.02E-02	2.02E-04	6.60E-03	PDGFC	A_23_P58396	1.58E-03	1.70E-02	8.3E-04	2.0E-01
KIAA1772	A_23_P119040	8.02E-02	2.04E-04	9.69E-03	RAB11FIP1	A_24_P945029	1.58E-03	1.70E-02	2.1E-04	7.9E-01
GJA4	A_23_P1083	8.02E-02	2.08E-04	2.17E-02	PLEC1	A_24_P913056	1.62E-03	1.72E-02	3.7E-04	4.5E-01
GRK5	A_23_P12884	8.02E-02	1.96E-04	3.31E-02	TPM1	A_24_P44462	1.69E-03	1.78E-02	4.8E-04	3.7E-01
PPP1R3B	A_23_P216199	8.02E-02	1.96E-04	7.57E-02	GPX7	A_24_P418816	1.86E-03	1.94E-02	1.7E-03	1.2E-01
GARNL3	A_24_P136522	8.02E-02	2.05E-04	1.02E-01	SPRR3	A_23_P62709	1.90E-03	1.95E-02	1.4E-03	1.4E-01
AL514561	A_32_P123176	8.02E-02	2.00E-04	1.55E-01	PPP2R2A	A_23_P123539	1.91E-03	1.95E-02	4.7E-03	4.3E-02
CCR7	A_23_P343398	8.02E-02	2.09E-04	2.93E-01	KDELR2	A_23_P19938	2.02E-03	2.04E-02	4.0E-03	5.4E-02
ICAM3	A_23_P164691	8.08E-02	2.12E-04	3.84E-01	PCOLCE	A_23_P251499	2.16E-03	2.16E-02	9.3E-04	2.5E-01
RNF32	A_23_P19816	8.31E-02	2.22E-04	6.80E-02	THBS2	A_24_P605612	2.23E-03	2.20E-02	3.2E-04	7.4E-01
DCX	A_23_P500328	8.31E-02	2.24E-04	9.73E-02	PDGFC	A_24_P163168	2.25E-03	2.21E-02	2.6E-02	9.3E-03
NAPSB	A_23_P90125	8.31E-02	2.27E-04	1.75E-01	NDUFV3	A_24_P416951	2.36E-03	2.29E-02	4.7E-03	5.5E-02
TPBG	A_23_P59261	8.31E-02	2.26E-04	5.61E-01	BASP1	A_23_P213385	2.40E-03	2.30E-02	2.9E-04	9.0E-01
RAMP3	A_23_P111737	8.54E-02	2.38E-04	1.64E-01	TRIM29	A_23_P340123	2.42E-03	2.30E-02	8.3E-04	3.2E-01
PGM5	A_24_P120907	8.54E-02	2.36E-04	5.04E-01	ADC	A_24_P11462	2.46E-03	2.32E-02	2.6E-03	1.0E-01
PECAM1	A_23_P252471	8.57E-02	2.46E-04	6.51E-02	LAMB3	A_23_P86012	2.51E-03	2.34E-02	7.5E-04	3.6E-01
PARP11	A_24_P188056	8.57E-02	2.42E-04	1.13E-01	COL4A1	A_24_P68342	2.53E-03	2.34E-02	9.9E-04	2.8E-01
LRAT	A_32_P113066	8.57E-02	2.46E-04	5.70E-01	SERPINB13	A_23_P432978	2.62E-03	2.39E-02	5.9E-03	4.9E-02

Supplementary Table 1. (continued)

FDR < 0.10 for survival of AC1					FDR based on Fisher combined p-value < 0.10 for N stage of AC1 + AC2					
Gene	Probe	FDR survival	p-value Survival	p-value Recurrence	Gene	Probe	Fisher's combined test FDR	Fisher's combined test p-value	p-value AC1	p-value AC2
C6orf182	A_24_P189112	8.59E-02	2.81E-04	9.95E-03	SLC2A4RG	A_24_P365442	2.67E-03	2.40E-02	3.8E-03	7.6E-02
POLR2A	A_24_P308128	8.59E-02	2.77E-04	1.64E-02	CNFN	A_23_P27473	2.69E-03	2.40E-02	7.4E-03	4.0E-02
C20orf160	A_23_P91414	8.59E-02	2.51E-04	1.76E-02	PRSS23	A_24_P937405	2.70E-03	2.40E-02	3.8E-04	7.8E-01
PLCG2	A_23_P106675	8.59E-02	2.80E-04	3.60E-02	COL3A1	A_24_P402242	2.76E-03	2.43E-02	3.4E-03	9.0E-02
KIAA2002	A_23_P65851	8.59E-02	2.89E-04	4.11E-02	MICAL2	A_23_P24843	2.77E-03	2.43E-02	3.4E-04	9.0E-01
SPARCL1	A_23_P113351	8.59E-02	2.79E-04	7.19E-02	UTP15	A_23_P213441	3.03E-03	2.63E-02	4.8E-04	7.1E-01
LRRTM4	A_24_P60268	8.59E-02	2.69E-04	7.39E-02	ADAMTS2	A_23_P213615	3.07E-03	2.64E-02	1.2E-03	2.8E-01
SDF2L1	A_23_P6344	8.59E-02	2.81E-04	8.47E-02	SLPI	A_23_P91230	3.22E-03	2.75E-02	1.3E-03	2.8E-01
CNR2	A_23_P310931	8.59E-02	2.94E-04	8.90E-02	PI3	A_23_P210465	3.41E-03	2.85E-02	5.9E-03	6.6E-02
PRSS12	A_23_P121637	8.59E-02	2.60E-04	9.17E-02	TRIO	A_23_P425880	3.41E-03	2.85E-02	4.9E-03	7.9E-02
IFT57	A_23_P121386	8.59E-02	2.62E-04	1.32E-01	AP2M1	A_23_P155624	3.50E-03	2.91E-02	9.6E-04	4.1E-01
PCDHA5	A_23_P334045	8.59E-02	2.83E-04	1.37E-01	PPP2CB	A_23_P134693	3.71E-03	3.05E-02	1.0E-02	4.1E-02
KIAA1909	A_23_P81640	8.59E-02	2.94E-04	1.75E-01	TRIO	A_24_P913431	3.73E-03	3.05E-02	8.7E-04	4.9E-01
TDRKH	A_24_P41975	8.59E-02	2.59E-04	1.88E-01	PCNT	A_23_P57347	3.83E-03	3.10E-02	6.8E-03	6.4E-02
TBCC	A_23_P251248	8.59E-02	2.69E-04	2.37E-01	DENND2D	A_23_P311346	4.14E-03	3.33E-02	5.2E-02	9.1E-03
FCRL3	A_23_P358438	8.59E-02	2.53E-04	2.43E-01	EMP1	A_24_P921446	4.20E-03	3.33E-02	3.8E-03	1.3E-01
CR620293	A_24_P854492	8.59E-02	2.92E-04	2.84E-01	TIMP2	A_23_P107401	4.21E-03	3.33E-02	2.6E-03	1.9E-01
CCND1	A_24_P124550	8.59E-02	2.85E-04	3.47E-01	C10orf116	A_23_P161439	4.29E-03	3.36E-02	3.4E-02	1.5E-02
THC2340670	A_32_P154121	8.59E-02	2.87E-04	4.21E-01	LOC147645	A_23_P101246	4.40E-03	3.43E-02	2.7E-02	1.9E-02
PUS3	A_23_P13073	8.59E-02	2.91E-04	5.10E-01	HOP	A_24_P913146	4.45E-03	3.44E-02	3.0E-02	1.7E-02
C6orf32	A_23_P215009	8.59E-02	2.90E-04	6.01E-01	FTH1	A_24_P58337	4.79E-03	3.67E-02	9.8E-04	5.8E-01
USHBP1	A_24_P366859	8.60E-02	2.99E-04	2.17E-02	SPINK7	A_23_P213832	4.93E-03	3.73E-02	1.8E-01	3.3E-03
CPEB3	A_23_P46813	8.60E-02	2.98E-04	7.99E-02	MYO10	A_24_P46357	4.95E-03	3.73E-02	1.6E-03	3.7E-01
NCF1	A_23_P42746	8.64E-02	3.03E-04	3.50E-01	PLCXD1	A_23_P61180	5.03E-03	3.75E-02	2.2E-02	2.7E-02
EIF5	A_24_P398810	8.69E-02	3.39E-04	1.15E-03	CREB3	A_23_P423389	5.05E-03	3.75E-02	6.8E-04	8.8E-01
TMEM87A	A_24_P65098	8.69E-02	3.38E-04	1.71E-02	CXorf56	A_23_P171223	5.25E-03	3.87E-02	8.4E-03	7.5E-02
A_32_P33434	A_32_P33434	8.69E-02	3.32E-04	6.24E-02	KLK12	A_23_P500010	5.41E-03	3.96E-02	3.5E-03	1.9E-01
KLRF1	A_32_P158966	8.69E-02	3.38E-04	7.73E-02	THBS2	A_23_P62021	5.88E-03	4.27E-02	7.8E-04	9.1E-01
TMEM24	A_23_P353056	8.69E-02	3.16E-04	8.33E-02	FBXL10	A_23_P87919	5.98E-03	4.31E-02	7.0E-03	1.0E-01
IRF4	A_23_P214360	8.69E-02	3.26E-04	1.15E-01	EIF4A2	A_32_P110751	6.23E-03	4.46E-02	2.1E-01	3.6E-03
AX775927	A_32_P148627	8.69E-02	3.31E-04	1.89E-01	FGFBP1	A_23_P30126	6.48E-03	4.61E-02	8.4E-02	9.4E-03
PAEP	A_23_P257129	8.69E-02	3.32E-04	2.41E-01	RGS5	A_23_P51518	6.84E-03	4.78E-02	1.5E-01	5.6E-03
VEGF	A_23_P81805	8.69E-02	3.22E-04	3.31E-01	C1orf42	A_23_P12155	6.88E-03	4.78E-02	2.1E-02	4.1E-02
DMXL1	A_24_P101128	8.69E-02	3.25E-04	4.05E-01	PSMD2	A_24_P42681	6.97E-03	4.78E-02	3.8E-03	2.3E-01
BCNP1	A_24_P940348	8.69E-02	3.39E-04	4.85E-01	ENY2	A_23_P82748	6.99E-03	4.78E-02	2.4E-03	3.6E-01
AK024456	A_24_P928281	8.69E-02	3.31E-04	5.05E-01	TPM2	A_23_P20566	7.11E-03	4.78E-02	3.1E-03	2.9E-01

Supplementary Table 1. (continued)

FDR < 0.10 for survival of AC1					FDR based on Fisher combined p-value < 0.10 for N stage of AC1 + AC2					
Gene	Probe	FDR survival	p-value Survival	p-value Recurrence	Gene	Probe	Fisher's combined test FDR	Fisher's combined test p-value	p-value AC1	p-value AC2
MLKL	A_24_P185044	8.69E-02	3.17E-04	5.55E-01	MYO10	A_23_P7596	7.12E-03	4.78E-02	3.3E-03	2.7E-01
DVL3	A_23_P218884	8.69E-02	3.17E-04	8.66E-01	PAM	A_24_P933704	7.14E-03	4.78E-02	1.1E-01	7.8E-03
PACIN1	A_23_P258088	8.69E-02	3.16E-04	9.36E-01	HPS3	A_23_P40817	7.18E-03	4.78E-02	1.2E-02	7.5E-02
ATP2A3	A_23_P207632	8.85E-02	3.48E-04	3.24E-01	EPOR	A_23_P367899	7.20E-03	4.78E-02	1.6E-03	5.8E-01
GIMAP6	A_23_P145631	8.85E-02	3.50E-04	4.49E-01	SLC22A16	A_24_P919084	7.21E-03	4.78E-02	3.9E-01	2.3E-03
ABL2	A_23_P138099	8.88E-02	3.56E-04	2.51E-01	FTH1	A_32_P111565	7.77E-03	5.10E-02	1.3E-03	7.8E-01
CCND1	A_23_P202837	8.88E-02	3.54E-04	4.23E-01	POF1B	A_23_P159764	7.80E-03	5.10E-02	1.1E-02	8.8E-02
AVPR2	A_23_P346798	8.91E-02	3.68E-04	8.51E-02	PCNT	A_24_P8350	8.08E-03	5.23E-02	7.7E-03	1.3E-01
ABHD7	A_23_P43898	8.91E-02	3.71E-04	1.17E-01	TBRG1	A_24_P21752	8.14E-03	5.23E-02	1.3E-01	7.7E-03
NCR3	A_23_P251881	8.91E-02	3.71E-04	1.81E-01	SLC7A1	A_24_P253251	8.29E-03	5.23E-02	2.0E-02	5.4E-02
SPIB	A_23_P39067	8.91E-02	3.63E-04	3.28E-01	SERPINB13	A_23_P119015	8.29E-03	5.23E-02	7.7E-03	1.4E-01
CES4	A_23_P374892	8.91E-02	3.70E-04	3.83E-01	DEFB4	A_23_P157628	8.31E-03	5.23E-02	2.1E-02	5.0E-02
SYNPO2	A_23_P310094	8.91E-02	3.70E-04	8.26E-01	KIFAP3	A_23_P62920	8.31E-03	5.23E-02	1.2E-03	8.8E-01
NAPSA	A_32_P107029	8.95E-02	3.75E-04	1.69E-01	S100A8	A_23_P434809	8.42E-03	5.27E-02	1.9E-02	5.8E-02
LAX1	A_24_P291278	9.06E-02	3.83E-04	1.55E-01	PDZK1IP1	A_23_P160920	8.56E-03	5.32E-02	4.2E-03	2.6E-01
SOX9	A_23_P26847	9.08E-02	3.86E-04	6.83E-01	MMP1	A_32_P429083	8.83E-03	5.45E-02	6.2E-01	1.8E-03
MMRN2	A_23_P150057	9.23E-02	3.95E-04	1.51E-02	IL8	A_32_P87013	8.99E-03	5.52E-02	2.0E-02	5.9E-02
ECSM2	A_23_P72651	9.26E-02	4.04E-04	1.88E-01	TAGLN	A_23_P87011	9.58E-03	5.84E-02	4.6E-02	2.7E-02
WDR31	A_23_P251324	9.26E-02	4.02E-04	2.04E-01	STXBP1	A_23_P135310	9.89E-03	5.94E-02	1.2E-02	1.1E-01
SP100	A_24_P916816	9.26E-02	4.01E-04	2.45E-01	C1orf42	A_24_P191047	9.90E-03	5.94E-02	1.4E-01	9.0E-03
A_32_P180185	A_32_P180185	9.26E-02	4.06E-04	5.83E-01	ADAMTS2	A_23_P321307	9.93E-03	5.94E-02	2.2E-03	5.9E-01
KCNA5	A_23_P417173	9.37E-02	4.15E-04	5.39E-02	GPSM3	A_24_P230521	1.02E-02	6.06E-02	3.4E-02	4.0E-02
THC2280976	A_32_P58437	9.37E-02	4.19E-04	7.52E-02	CLDN7	A_23_P164284	1.03E-02	6.06E-02	5.3E-03	2.6E-01
LOC646686	A_24_P937649	9.37E-02	4.18E-04	8.54E-02	SLC2A4RG	A_23_P102571	1.03E-02	6.06E-02	1.7E-02	8.0E-02
TMEM105	A_32_P919718	9.37E-02	4.23E-04	2.12E-01	SULT2B1	A_23_P107981	1.05E-02	6.10E-02	2.3E-02	6.0E-02
ENST00000371030	A_32_P206479	9.37E-02	4.21E-04	3.02E-01	SMS	A_24_P305764	1.05E-02	6.10E-02	4.9E-02	2.8E-02
AL525862	A_32_P97046	9.38E-02	4.32E-04	1.48E-02	SAPS1	A_23_P119448	1.06E-02	6.10E-02	3.0E-01	4.6E-03
LOC441208	A_24_P145009	9.38E-02	4.43E-04	2.18E-02	RPL37A	A_23_P142724	1.07E-02	6.17E-02	4.0E-02	3.6E-02
KCNA3	A_23_P201138	9.38E-02	4.39E-04	2.41E-02	KDELRL2	A_23_P19936	1.08E-02	6.18E-02	6.0E-03	2.4E-01
CFP	A_23_P22444	9.38E-02	4.31E-04	3.37E-01	COL4A1	A_23_P65240	1.09E-02	6.18E-02	1.7E-03	8.5E-01
PRKCB1	A_23_P206585	9.38E-02	4.40E-04	4.04E-01	SEMA3C	A_23_P256473	1.10E-02	6.18E-02	5.7E-03	2.6E-01
CLEC10A	A_23_P141505	9.38E-02	4.36E-04	5.96E-01	FSTL1	A_23_P212696	1.11E-02	6.18E-02	2.9E-03	5.0E-01
RNF36	A_24_P50543	9.38E-02	4.30E-04	7.60E-01	DSG3	A_23_P153120	1.11E-02	6.18E-02	2.1E-02	7.1E-02
SMARCA3	A_24_P277155	9.38E-02	4.43E-04	9.02E-01	IVL	A_23_P353524	1.15E-02	6.37E-02	7.2E-02	2.1E-02
ENST00000377515	A_23_P361679	9.40E-02	4.59E-04	5.83E-03	ARL14	A_23_P92161	1.18E-02	6.49E-02	2.4E-03	6.6E-01
DDIT4	A_23_P104318	9.40E-02	4.61E-04	3.16E-02	MLLT7	A_23_P217487	1.22E-02	6.68E-02	7.0E-01	2.3E-03

Supplementary Table 1. (continued)

FDR < 0.10 for survival of AC1					FDR based on Fisher combined p-value < 0.10 for N stage of AC1 + AC2					
Gene	Probe	FDR survival	p-value Survival	p-value Recurrence	Gene	Probe	Fisher's combined test FDR	Fisher's combined test p-value	p-value AC1	p-value AC2
C1orf67	A_32_P87531	9.40E-02	4.67E-04	4.94E-02	SEMA4D	A_24_P261169	1.28E-02	7.00E-02	1.0E-02	1.7E-01
ENST00000311695	A_32_P188825	9.40E-02	4.57E-04	8.48E-02	SLC9A3R1	A_23_P308519	1.29E-02	7.01E-02	3.9E-03	4.6E-01
ZNF573	A_23_P339079	9.40E-02	4.66E-04	1.12E-01	DMKN	A_23_P320261	1.30E-02	7.03E-02	2.8E-02	6.3E-02
BC032907	A_24_P870362	9.40E-02	4.57E-04	1.19E-01	MGC3207	A_24_P279797	1.36E-02	7.26E-02	7.0E-03	2.7E-01
THC2407434	A_24_P565390	9.40E-02	4.51E-04	1.76E-01	AK021531	A_24_P503729	1.36E-02	7.26E-02	7.0E-03	2.7E-01
ENST00000374472	A_32_P48054	9.40E-02	4.64E-04	1.83E-01	HOP	A_23_P254507	1.37E-02	7.29E-02	2.5E-02	7.6E-02
GIMAP8	A_24_P132383	9.40E-02	4.58E-04	4.53E-01	PDE4DIP	A_24_P253100	1.39E-02	7.33E-02	4.7E-03	4.0E-01
AK056689	A_24_P548060	9.63E-02	4.81E-04	1.56E-01	SLPI	A_24_P190472	1.40E-02	7.33E-02	5.9E-03	3.2E-01
FAM27E2	A_24_P458479	9.64E-02	4.89E-04	3.67E-02	POF1B	A_24_P250815	1.41E-02	7.38E-02	2.6E-02	7.5E-02
ZC3H12D	A_24_P187826	9.64E-02	4.85E-04	1.11E-01	AEBP1	A_23_P157299	1.42E-02	7.40E-02	1.2E-02	1.6E-01
NCF1	A_32_P116203	9.64E-02	4.88E-04	3.85E-01	RAB25	A_23_P115091	1.43E-02	7.40E-02	6.8E-03	2.9E-01
HOXB9	A_23_P27013	9.65E-02	4.98E-04	1.26E-02	GPX7	A_23_P73972	1.46E-02	7.53E-02	1.2E-02	1.8E-01
TSPAN19	A_23_P2322	9.65E-02	4.92E-04	2.27E-02	YWHAH	A_23_P103070	1.49E-02	7.61E-02	1.3E-02	1.6E-01
M69012	A_24_P127159	9.65E-02	4.97E-04	9.75E-02	DKK3	A_24_P261417	1.49E-02	7.61E-02	3.8E-03	5.5E-01
TANC2	A_23_P218346	9.65E-02	4.99E-04	2.15E-01	DKK3	A_23_P162047	1.51E-02	7.64E-02	2.7E-03	7.7E-01
THC2308938	A_32_P99032	9.67E-02	5.06E-04	2.11E-01	EPPK1	A_23_P83388	1.59E-02	7.96E-02	6.0E-03	3.7E-01
CCL21	A_23_P112470	9.67E-02	5.04E-04	2.43E-01	TPM1	A_23_P363344	1.60E-02	7.96E-02	1.6E-01	1.4E-02
WDR68	A_23_P422268	9.84E-02	5.31E-04	4.83E-02	AKR1B10	A_23_P93641	1.60E-02	7.96E-02	5.0E-02	4.5E-02
ENST00000377492	A_23_P348979	9.84E-02	5.31E-04	7.30E-02	KRT2	A_23_P116850	1.60E-02	7.96E-02	4.2E-02	5.3E-02
RG55	A_23_P46045	9.84E-02	5.31E-04	1.23E-01	AGPAT2	A_32_P26103	1.62E-02	7.99E-02	7.6E-03	3.0E-01
CCL15	A_23_P218369	9.84E-02	5.27E-04	1.79E-01	TMEM40	A_23_P29551	1.62E-02	7.99E-02	1.7E-01	1.4E-02
CCR6	A_24_P234921	9.84E-02	5.34E-04	2.00E-01	LLGL2	A_23_P129738	1.68E-02	8.18E-02	1.4E-02	1.7E-01
DARC	A_23_P115161	9.84E-02	5.41E-04	2.78E-01	RPL37A	A_32_P783	1.69E-02	8.18E-02	2.6E-02	9.1E-02
CD79B	A_23_P207201	9.84E-02	5.40E-04	2.83E-01	CALD1	A_24_P255524	1.69E-02	8.18E-02	6.4E-03	3.7E-01
GPCR5C	A_23_P346670	9.84E-02	5.41E-04	3.66E-01	DUOX1	A_24_P316586	1.72E-02	8.26E-02	9.8E-02	2.5E-02
LY9	A_24_P324674	9.84E-02	5.18E-04	5.99E-01	LEPREL2	A_23_P87752	1.72E-02	8.26E-02	4.3E-01	5.8E-03
HSH2D	A_23_P153372	9.84E-02	5.34E-04	7.05E-01	FADS3	A_23_P64404	1.85E-02	8.83E-02	6.6E-03	4.0E-01
BC044628	A_32_P117453	9.89E-02	5.51E-04	4.05E-03	IMPDH2	A_24_P166042	1.88E-02	8.90E-02	2.0E-02	1.4E-01
PRAME	A_24_P216361	9.89E-02	5.53E-04	1.09E-02	FTH1	A_32_P342064	1.88E-02	8.90E-02	2.9E-03	9.5E-01
MMRN1	A_23_P18539	9.89E-02	5.54E-04	2.12E-01	RBP7	A_24_P165423	1.94E-02	9.15E-02	5.3E-02	5.4E-02
ZBP1	A_23_P259141	9.89E-02	5.51E-04	3.55E-01	HTRA1	A_23_P97990	1.97E-02	9.21E-02	4.3E-03	6.7E-01
ARHGEF15	A_24_P359007	9.89E-02	5.64E-04	6.66E-03	PRKAB2	A_24_P917711	2.01E-02	9.35E-02	2.2E-02	1.3E-01
ERGIC1	A_24_P97770	9.89E-02	5.67E-04	7.28E-03	FTH1	A_32_P820503	2.02E-02	9.36E-02	3.9E-03	7.6E-01
PCDHA1	A_24_P146138	9.89E-02	5.67E-04	4.35E-02	PTK6	A_23_P56978	2.04E-02	9.40E-02	3.1E-01	9.7E-03
ZNF540	A_23_P90542	9.89E-02	5.70E-04	5.78E-02	FLJ23447	A_23_P433798	2.05E-02	9.40E-02	3.5E-03	8.5E-01
ENST00000381158	A_32_P77831	9.89E-02	5.71E-04	1.17E-01	C9orf5	A_24_P12904	2.09E-02	9.56E-02	1.1E-02	2.8E-01

Supplementary Table 1. (continued)

FDR < 0.10 for survival of AC1					FDR based on Fisher combined p-value < 0.10 for N stage of AC1 + AC2					
Gene	Probe	FDR survival	p-value Survival	p-value Recurrence	Gene	Probe	Fisher's combined test FDR	Fisher's combined test p-value	p-value AC1	p-value AC2
CAMK2N1	A_24_P117620	9.89E-02	5.73E-04	1.58E-01	S100A9	A_23_P23048	2.15E-02	9.78E-02	2.4E-02	1.3E-01
CCDC69	A_24_P97825	9.89E-02	5.59E-04	5.16E-01	RHO	A_23_P57950	2.16E-02	9.78E-02	7.3E-03	4.4E-01
IL27RA	A_23_P27606	9.89E-02	5.75E-04	5.40E-01	KLK7	A_23_P39056	2.20E-02	9.89E-02	9.9E-02	3.3E-02
BLR1	A_24_P252945	9.92E-02	5.79E-04	2.30E-01	EPOR	A_23_P381954	2.20E-02	9.89E-02	4.4E-03	7.4E-01
FAM112A	A_23_P57020	9.95E-02	5.84E-04	2.56E-01	COL7A1	A_23_P144071	2.23E-02	9.98E-02	2.6E-02	1.3E-01
ZBTB34	A_24_P238365	9.99E-02	5.96E-04	2.12E-01	-	-	-	-	-	-
STC2	A_23_P416395	9.99E-02	5.97E-04	2.36E-01	-	-	-	-	-	-
INSIG2	A_23_P102454	9.99E-02	5.94E-04	4.59E-01	-	-	-	-	-	-
U09197	A_24_P937240	9.99E-02	5.99E-04	5.16E-01	-	-	-	-	-	-
EXOC6	A_23_P169576	9.99E-02	5.90E-04	9.45E-01	-	-	-	-	-	-

Supplementary Table 2. Selected gene signature and qPCR assays

Type of gene	Ensembl gene ID	Chromosome name	Band	Associated Gene name	Description	Taqman assay technical validation (TLDA.v1)	Taqman assay final signature (after technical validation) (TLDA.v2)
LNMsig	ENSG00000148848	10	q26.2	ADAM12	ADAM metalloproteinase domain 12 [Source:HGNC Symbol;Acc:HGNC:190]	Hs01106101_m1	Hs01106101_m1
Ossig	ENSG00000129467	14	q12	ADCY4	adenylate cyclase 4 [Source:HGNC Symbol;Acc:HGNC:235]	Hs00934099_m1	Hs00934099_m1
Ossig	ENSG00000116748	1	p13.2	AMPD1	adenosine monophosphate deaminase 1 [Source:HGNC Symbol;Acc:HGNC:468]	Hs00921502_m1	Hs00921502_m1
Ossig	ENSG00000109321	4	q13.3	AREG	amphiregulin [Source:HGNC Symbol;Acc:HGNC:651]	Hs00950669_m1	Hs00950669_m1
Ossig	ENSG00000118520	6	q23.2	ARG1	arginase 1 [Source:HGNC Symbol;Acc:HGNC:663]	NA	Hs00968979_m1
Ossig	ENSG00000033627	17	q21.2	ATP6V0A1	ATPase, H+ transporting, lysosomal V0 subunit a1 [Source:HGNC Symbol;Acc:HGNC:865]	Hs00193110_m1	Hs00193110_m1
Ossig	ENSG00000160345	9	q34.3	C9orf116	chromosome 9 open reading frame 116 [Source:HGNC Symbol;Acc:HGNC:28435]	Hs01077891_m1	Hs01077891_m1
Ossig	ENSG00000179058	9	q34.11	C9orf50	chromosome 9 open reading frame 50 [Source:HGNC Symbol;Acc:HGNC:23677]	Hs01368756_m1	NA
Ossig/ LNMsig	ENSG00000122786	7	q33	CALD1	caldesmon 1 [Source:HGNC Symbol;Acc:HGNC:1441]	Hs00921982_m1	Hs00921982_m1
Ossig	ENSG00000129993	16	q24.3	CBFA2T3	core-binding factor, runt domain, alpha subunit 2; translocated to, 3 [Source:HGNC Symbol;Acc:HGNC:1537]	NA	Hs00602520_m1
Ossig	ENSG00000168071	11	q13.1	CCDC88B	coiled-coil domain containing 88B [Source:HGNC Symbol;Acc:HGNC:26757]	Hs00989954_mH	Hs00989954_mH
Ossig/ LNMsig	ENSG00000110092	11	q13.3	CCND1	cyclin D1 [Source:HGNC Symbol;Acc:HGNC:1582]	Hs00765553_m1	Hs00765553_m1
Ossig	ENSG00000136807	9	q34.11	CDK9	cyclin-dependent kinase 9 [Source:HGNC Symbol;Acc:HGNC:1780]	Hs00977896_g1	NA
Ossig	ENSG00000147889	9	p21.3	CDKN2A	cyclin-dependent kinase inhibitor 2A [Source:HGNC Symbol;Acc:HGNC:1787]	NA	Hs00923894_m1

Supplementary Table 2. (continued)

Type of gene	Ensembl gene ID	Chromosome name	Band	Associated Gene name	Description	Taqman assay technical validation (TLDA.v1)	Taqman assay final signature (after technical validation) (TLDA.v2)
Ossig	ENSG00000163815	3	p21.31	CLEC3B	C-type lectin domain family 3, member B [Source:HGNC Symbol;Acc:HGNC:11891]	Hs00162844_m1	Hs00162844_m1
LNMsig	ENSG00000060718	1	p21.1	COL11A1	collagen, type XI, alpha 1 [Source:HGNC Symbol;Acc:HGNC:2186]	Hs01097664_m1	Hs01097664_m1
Ossig	ENSG00000188153	X	q22.3	COL4A5	collagen, type IV, alpha 5 [Source:HGNC Symbol;Acc:HGNC:2207]	Hs00166712_m1	Hs00166712_m1
LNMsig	ENSG00000130635	9	q34.3	COL5A1	collagen, type V, alpha 1 [Source:HGNC Symbol;Acc:HGNC:2209]	Hs00609133_m1	Hs00609133_m1
LNMsig	ENSG00000142156	21	q22.3	COL6A1	collagen, type VI, alpha 1 [Source:HGNC Symbol;Acc:HGNC:2211]	Hs01095585_m1	Hs01095585_m1
Ossig	ENSG00000085733	11	q13.3	CTTN	cortactin [Source:HGNC Symbol;Acc:HGNC:3338]	Hs01124225_m1	Hs01124225_m1
Ossig	ENSG00000156234	4	q21.1	CXCL13	chemokine (C-X-C motif) ligand 13 [Source:HGNC Symbol;Acc:HGNC:10639]	Hs00757930_m1	Hs00757930_m1
LNMsig	ENSG00000176797	8	p23.1	DEFB103A	defensin, beta 103A [Source:HGNC Symbol;Acc:HGNC:15967]	Hs00218678_m1	Hs00218678_m1
Ossig	ENSG00000100664	14	q32.32	EIF5	eukaryotic translation initiation factor 5 [Source:HGNC Symbol;Acc:HGNC:3299]	Hs01028813_g1	Hs01028813_g1
LNMsig	ENSG00000110723	11	q22.3	EXPH5	exophilin 5 [Source:HGNC Symbol;Acc:HGNC:30578]	Hs00323579_m1	Hs00323579_m1
LNMsig	ENSG00000115414	2	q35	FN1	fibronectin 1 [Source:HGNC Symbol;Acc:HGNC:3778]	Hs00415008_m1	Hs00415008_m1
HKG	ENSG00000111640	12	p13.31	GAPDH	glyceraldehyde-3-phosphate dehydrogenase [Source:HGNC Symbol;Acc:HGNC:4141]	Hs99999905_m1	Hs99999905_m1
HKG	ENSG00000169919	7	q11.21	GUSB	glucuronidase, beta [Source:HGNC Symbol;Acc:HGNC:4696]	Hs00939627_m1	Hs00939627_m1
LNMsig	ENSG00000169429	4	q13.3	IL8	interleukin 8 [Source:HGNC Symbol;Acc:HGNC:6025]	Hs00174103_m1	Hs00174103_m1
Ossig	ENSG00000163083	2	q14.2	INHBB	inhibin, beta B [Source:HGNC Symbol;Acc:HGNC:6067]	Hs00173582_m1	Hs00173582_m1

Supplementary Table 2. (continued)

Type of gene	Ensembl gene ID	Chromosome name	Band	Associated Gene name	Description	Taqman assay technical validation (TLDA.v1)	Taqman assay final signature (after technical validation) (TLDA.v2)
Ossig	ENSG00000176842	16	q12.2	IRX5	iroquois homeobox 5 [Source:HGNC Symbol;Acc:HGNC:14361]	Hs04334749_m1	Hs04334749_m1
Ossig	ENSG00000174718	12	p11.21	KIAA1551	KIAA1551 [Source:HGNC Symbol;Acc:HGNC:25559]	Hs01028589_m1	Hs01028589_m1
Ossig	ENSG00000134545	12	p13.2	KLRC1	killer cell lectin-like receptor subfamily C, member 1 [Source:HGNC Symbol;Acc:HGNC:6374]	Hs00970274_m1	Hs00970274_m1
LNMsig	ENSG00000118058	11	q23.3	KMT2A	lysine (K)-specific methyltransferase 2A [Source:HGNC Symbol;Acc:HGNC:7132]	Hs00610538_m1	Hs00610538_m1
LNMsig	ENSG00000108244	17	q21.2	KRT23	keratin 23, type I [Source:HGNC Symbol;Acc:HGNC:6438]	Hs00210096_m1	Hs00210096_m1
Ossig	ENSG00000204583	12	q24.33	LRCOL1	leucine rich colipase-like 1 [Source:HGNC Symbol;Acc:HGNC:44160]	Hs01113075_m1	Hs01113075_m1
LNMsig	ENSG00000139329	12	q21.33	LUM	lumican [Source:HGNC Symbol;Acc:HGNC:6724]	Hs00929860_m1	Hs00929860_m1
LNMsig	ENSG00000213401	X	q28	MAGEA12	melanoma antigen family A, 12 [Source:HGNC Symbol;Acc:HGNC:6799]	Hs04176236_m1	NA
LNMsig	ENSG00000149573	11	q23.3	MPZL2	myelin protein zero-like 2 [Source:HGNC Symbol;Acc:HGNC:3496]	Hs01083647_m1	Hs01083647_m1
Ossig	ENSG00000133055	1	q32.1	MYBPH	myosin binding protein H [Source:HGNC Symbol;Acc:HGNC:7552]	Hs00192226_m1	Hs00192226_m1
Ossig	ENSG00000133026	17	p13.1	MYH10	myosin, heavy chain 10, non-muscle [Source:HGNC Symbol;Acc:HGNC:7568]	Hs00992055_m1	NA
Ossig	ENSG00000104419	8	q24.22	NDRG1	N-myc downstream regulated 1 [Source:HGNC Symbol;Acc:HGNC:7679]	Hs00608387_m1	Hs00608387_m1
LNMsig	ENSG00000122884	10	q22.1	P4HA1	prolyl 4-hydroxylase, alpha polypeptide I [Source:HGNC Symbol;Acc:HGNC:8546]	Hs00914594_m1	Hs00914594_m1
Ossig	ENSG00000110435	11	p13	PDHX	pyruvate dehydrogenase complex, component X [Source:HGNC Symbol;Acc:HGNC:21350]	Hs00185790_m1	Hs00185790_m1
Ossig	ENSG00000154330	9	q21.11	PGM5	phosphoglucomutase 5 [Source:HGNC Symbol;Acc:HGNC:8908]	Hs00222671_m1	Hs00222671_m1

Supplementary Table 2. (continued)

Type of gene	Ensembl gene ID	Chromosome name	Band	Associated Gene name	Description	Taqman assay technical validation (TLDA.v1)	Taqman assay final signature (after technical validation) (TLDA.v2)
Ossig	ENSG00000110777	11	q23.1	POU2AF1	POU class 2 associating factor 1 [Source:HGNC Symbol;Acc:HGNC:9211]	NA	Hs01573371_m1
Ossig	ENSG00000185686	22	q11.22	PRAME	preferentially expressed antigen in melanoma [Source:HGNC Symbol;Acc:HGNC:9336]	Hs01022301_m1	Hs01022301_m1
Ossig	ENSG00000127329	12	q15	PTPRB	protein tyrosine phosphatase, receptor type, B [Source:HGNC Symbol;Acc:HGNC:9665]	Hs01549049_m1	Hs01549049_m1
LNMsig	ENSG00000143248	1	q23.3	RGS5	regulator of G-protein signaling 5 [Source:HGNC Symbol;Acc:HGNC:10001]	Hs01555176_m1	Hs01555176_m1
HKG	ENSG00000174444	15	q22.31	RPL4	ribosomal protein L4 [Source:HGNC Symbol;Acc:HGNC:10353]	Hs03044647_g1	Hs03044647_g1
HKG	ENSG00000089157	12	q24.23	RPLP0	ribosomal protein, large, P0 [Source:HGNC Symbol;Acc:HGNC:10371]	Hs99999902_m1	Hs99999902_m1
LNMsig	ENSG00000166922	15	q13.3	SCG5	secretogranin V [Source:HGNC Symbol;Acc:HGNC:10816]	Hs00161638_m1	Hs00161638_m1
Ossig	ENSG00000007908	1	q24.2	SELE	selectin E [Source:HGNC Symbol;Acc:HGNC:10718]	Hs00950401_m1	Hs00950401_m1
Ossig	ENSG00000174175	1	q24.2	SELP	selectin P (granule membrane protein 140kDa, antigen CD62) [Source:HGNC Symbol;Acc:HGNC:10721]	Hs00927900_m1	Hs00927900_m1
LNMsig	ENSG00000197632	18	q21.33	SERPINB2	serpin peptidase inhibitor, clade B (ovalbumin), member 2 [Source:HGNC Symbol;Acc:HGNC:8584]	Hs01010736_m1	Hs01010736_m1
LNMsig	ENSG00000149257	11	q13.5	SERPINH1	serpin peptidase inhibitor, clade H (heat shock protein 47), member 1, (collagen binding protein 1) [Source:HGNC Symbol;Acc:HGNC:1546]	NA	Hs01060397_g1
Ossig	ENSG00000148942	11	p14.2	SLC5A12	solute carrier family 5 (sodium/monocarboxylate cotransporter), member 12 [Source:HGNC Symbol;Acc:HGNC:28750]	Hs01054637_m1	Hs01054637_m1
Ossig	ENSG00000198021	X	q27.2	SPANXA1	sperm protein associated with the nucleus, X-linked, family member A1 [Source:HGNC Symbol;Acc:HGNC:11218]	Hs03007483_gH	Hs03007483_gH

Supplementary Table 2. (continued)

Type of gene	Ensembl gene ID	Chromosome name	Band	Associated Gene name	Description	Taqman assay technical validation (TLDA.v1)	Taqman assay final signature (after technical validation) (TLDA.v2)
Ossig	ENSG00000122711	9	p13.3	SPINK4	serine peptidase inhibitor, Kazal type 4 [Source:HGNC Symbol;Acc:HGNC:16646]	Hs00205508_m1	NA
LNMsig	ENSG00000152377	5	q31.2	SPOCK1	sparc/osteonectin, cwcv and kazal-like domains proteoglycan (testican) 1 [Source:HGNC Symbol;Acc:HGNC:11251]	Hs00928769_m1	Hs00928769_m1
Ossig	ENSG00000159516	1	q21.3	SPRR2G	small proline-rich protein 2G [Source:HGNC Symbol;Acc:HGNC:11267]	Hs00972901_s1	Hs00972901_s1
Ossig	ENSG00000172403	4	q26	SYNPO2	synaptopodin 2 [Source:HGNC Symbol;Acc:HGNC:17732]	Hs00326493_m1	Hs00326493_m1
Ossig	ENSG00000170921	17	q23.2	TANC2	tetratricopeptide repeat, ankyrin repeat and coiled-coil containing 2 [Source:HGNC Symbol;Acc:HGNC:30212]	Hs00229073_m1	Hs00229073_m1
Ossig	ENSG00000100721	14	q32.13	TCL1A	T-cell leukemia/lymphoma 1A [Source:HGNC Symbol;Acc:HGNC:11648]	NA	Hs00951350_m1
LNMsig	ENSG00000150779	11	q23.1	TIMM8B	translocase of inner mitochondrial membrane 8 homolog B (yeast) [Source:HGNC Symbol;Acc:HGNC:11818]	Hs02339636_g1	Hs02339636_g1
Ossig	ENSG00000114854	3	p21.1	TNNC1	troponin C type 1 (slow) [Source:HGNC Symbol;Acc:HGNC:11943]	Hs00896999_g1	Hs00896999_g1
Ossig	ENSG00000168477	6	p21.32	TNXB	tenascin XB [Source:HGNC Symbol;Acc:HGNC:11976]	Hs00954865_m1	Hs00954865_m1
Ossig	ENSG00000146242	6	q14.1	TPBG	trophoblast glycoprotein [Source:HGNC Symbol;Acc:HGNC:12004]	Hs00907219_m1	NA
LNMsig	ENSG00000140416	15	q22.2	TPM1	tropomyosin 1 (alpha) [Source:HGNC Symbol;Acc:HGNC:12010]	Hs00165966_m1	Hs00165966_m1
Ossig	ENSG00000110900	12	p11.21	TSPAN11	tetraspanin 11 [Source:HGNC Symbol;Acc:HGNC:30795]	Hs01391666_m1	Hs01391666_m1
Ossig	ENSG00000112715	6	p21.1	VEGFA	vascular endothelial growth factor A [Source:HGNC Symbol;Acc:HGNC:12680]	Hs00900055_m1	Hs00900055_m1

Supplementary Table 3. Pearson's correlation coefficients and corresponding p-values of technical validation

Gene	Correlation coefficient PCR vs Array	P-value correlation
SPRR2G	-0.98	2.30E-13
SERPINB2	-0.95	1.30E-10
MYBPH	-0.94	4.90E-10
TNNC1	-0.94	8.10E-10
KRT23	-0.93	1.90E-09
CXCL13	-0.93	4.20E-09
IL8	-0.93	1.50E-08
COL11A1	-0.9	9.10E-08
DEFB103	-0.89	1.30E-07
SYNPO2	-0.88	4.00E-07
PRAME	-0.87	5.10E-07
AREG	-0.87	7.20E-07
TIMM8B	-0.86	1.10E-06
PDHX	-0.86	1.50E-06
AMPD1	-0.86	1.50E-06
SPANXA	-0.85	1.90E-06
FN1	-0.85	2.40E-06
SPOCK1	-0.83	5.50E-06
EXPH5	-0.81	1.30E-05
KLRC1	-0.81	1.30E-05
SLC5A12	-0.8	2.00E-05
COL5A1	-0.8	2.70E-05
LUM	-0.79	2.80E-05
TSPAN11	-0.76	8.50E-05
SELE	-0.76	9.60E-05
TPM1	-0.73	2.70E-04
INHBB	-0.7	5.80E-04
MPZL2	-0.7	6.40E-04
CLEC3B	-0.69	7.40E-04
CCND1	-0.68	9.80E-04
TNXB	-0.67	1.10E-03
NDRG1	-0.67	1.30E-03
CTTN	-0.67	1.40E-03
ADAM12	-0.64	2.30E-03
SCG5	-0.64	2.40E-03
KIAA1551	-0.64	2.40E-03
P4HA1	-0.61	4.10E-03
CALD1	-0.57	8.40E-03
ADCY4	-0.56	9.50E-03
SELP	-0.56	1.00E-02
VEGFA	-0.56	1.00E-02
COL4A5	-0.54	1.40E-02
KMT2A	-0.53	1.70E-02
RGSS	-0.52	1.90E-02

Supplementary Table 3. (continued)

Gene	Correlation coefficient PCR vs Array	P-value correlation
C9orf116	-0.51	2.20E-02
TANC2	-0.5	2.30E-02
PGM5	-0.48	3.30E-02
LRCOL1	-0.45	4.50E-02
COL6A1	-0.45	4.90E-02
PTPRB	-0.44	5.00E-02
CCDC88B	-0.42	6.30E-02
IRX5	-0.4	8.30E-02
MAGEA12 ^a	-0.37	1.10E-01
TPBG ^a	-0.22	3.50E-01
ATP6V0A1 ^a	-0.21	3.80E-01
C9orf50 ^a	-0.21	4.00E-01
CDK9 ^a	-0.17	4.70E-01
SPINK4 ^a	0.15	5.30E-01
MYH10 ^a	-0.07	7.50E-01
EIF5 ^a	0.03	8.90E-01

^a. Genes with correlation coefficients ≤ 1 SD (mean $r=0.64$, $SD=0.26$)

Supplementary Table 4. Coefficient estimates and false discovery rates of qPCR results of the gene signatures

Gene	Overall survival					Lymph node metastasis					Disease free survival				
	Univariate estimate	Estimate 95%CI	p-value	FDR	Ridge estimate ^a	Univariate estimate	Estimate 95%CI	p-value	FDR	Ridge estimate ^a	Univariate estimate	Estimate 95%CI	p-value	FDR	Ridge estimate ^a
ADAM12	-0.05	-0.27	0.17	0.66		-0.25	-0.52	0.01	0.07	0.10	2.1E-02	-0.05	-0.28	0.18	0.67
ADCY4	0.45	0.14	0.76	4.6E-03	0.03	0.04	0.38	-0.02	0.82	0.07		0.53	0.20	0.86	1.8E-03
AMPD1	0.08	-0.02	0.17	0.12	0.26	4.4E-03	-0.04	-0.16	0.08	0.53		0.07	-0.04	0.17	0.20
AREG	-0.01	-0.18	0.16	0.93	0.95	4.4E-03	-0.22	-0.45	-0.01	0.05		-0.14	-0.33	0.06	0.16
ARG1	0.01	-0.07	0.09	0.82	0.87	-5.6E-04	0.12	0.03	0.23	0.02		-0.03	-0.12	0.05	0.40
ATP6V0A1	0.10	-0.28	0.48	0.61	0.82	0.01	0.32	-0.12	0.80	0.17		0.09	-0.31	0.50	0.64
C9orf116	-0.30	-0.60	0.00	0.05	0.12	-0.05	-0.21	-0.57	0.14	0.25		-0.29	-0.61	0.03	0.08
CALD1	-0.01	-0.35	0.34	0.98	0.98	-0.01	-0.51	-0.96	-0.09	0.02	0.04	-0.1	-0.16	-0.52	0.20
CBFA2T3	0.47	0.20	0.73	5.4E-04	0.01	0.04	0.36	0.03	0.70	0.03		0.50	0.23	0.76	2.5E-04
CCDC88B	0.31	0.02	0.59	0.03	0.11	0.03	0.25	-0.07	0.59	0.13		0.44	0.15	0.73	2.9E-03
CCND1	-0.08	-0.29	0.14	0.48	0.67	-1.5E-03	-0.25	-0.54	0.02	0.08	0.11	-0.1	-0.13	-0.37	0.10
CDKN2A	0.02	-0.08	0.11	0.71	0.84	0.01	-0.06	-0.17	0.06	0.32		0.01	-0.09	0.11	0.81
CLEC3B	0.25	0.01	0.50	0.04	0.12	0.02	0.44	0.14	0.77	0.01		0.38	0.12	0.65	4.2E-03
COL11A1	-0.10	-0.22	0.02	0.11			-0.10	-0.23	0.03	0.15	0.17	2.8E-02	-0.07	-0.19	0.06
COL4A5	-0.11	-0.32	0.11	0.34	0.54	-0.02	-0.20	-0.49	0.07	0.16		-0.10	-0.34	0.13	0.38
COL5A1	-0.08	-0.31	0.14	0.45			-0.30	-0.58	-0.03	0.03	0.06	-1.2E-02	-0.17	-0.41	0.06
COL6A1	-0.02	-0.29	0.25	0.88			-0.24	-0.56	0.07	0.14	0.17	3.3E-02	-0.03	-0.31	0.25
CTTN	-0.11	-0.33	0.10	0.30	0.52	-0.02	0.09	-0.18	0.36	0.51		-0.25	-0.47	-0.03	0.03
CXCL13	0.16	0.02	0.29	0.02	0.09	0.02	0.09	-0.08	0.26	0.30		0.12	-0.02	0.26	0.09
DEFB103	0.06	-0.02	0.14	0.12			0.13	0.03	0.24	0.02	0.04	0.1	-0.03	-0.12	0.06
EIF5	0.15	-0.26	0.56	0.48	0.67	0.02	-0.01	-0.47	0.46	0.98		0.13	-0.30	0.57	0.55
EXPH5	0.26	-0.02	0.53	0.07			0.54	0.23	0.89	1.1E-03	0.01	0.1	0.18	-0.11	0.46
FN1	-0.13	-0.30	0.04	0.14			-0.40	-0.65	-0.17	9.3E-04	0.01	-0.1	-0.21	-0.40	-0.03
IL8	-0.13	-0.30	0.04	0.15			-0.09	-0.28	0.10	0.34	0.38	-3E-02	-0.16	-0.34	0.03
INHBB	-0.05	-0.26	0.17	0.66	0.83	-0.03	-0.04	-0.31	0.24	0.80		0.03	-0.19	0.25	0.78
IRX5	0.10	-0.16	0.37	0.45	0.66	0.02	0.16	-0.15	0.48	0.31		0.18	-0.11	0.47	0.23
KIAA1551	0.33	0.00	0.66	0.05	0.12	0.04	0.22	-0.14	0.61	0.24		0.24	-0.10	0.58	0.17
KLRC1	0.14	0.01	0.28	0.03	0.11	0.03	-0.17	-0.37	0.02	0.09		0.09	-0.06	0.25	0.24
KMT2A	0.32	-0.17	0.81	0.20			0.15	-0.40	0.70	0.59	0.59	4.2E-02	0.27	-0.23	0.76
KRT23	-0.01	-0.14	0.12	0.92			0.27	0.10	0.47	2.8E-03	0.02	0.1	-0.03	-0.16	0.11
LRCOL1	0.19	0.08	0.30	5.3E-04	0.01	0.08	-0.05	-0.19	0.08	0.43		0.13	0.02	0.25	0.03
LUM	0.02	-0.24	0.28	0.89			-0.14	-0.46	0.16	0.37	0.39	-8.9E-03	0.11	-0.14	0.37
MPZL2	0.26	0.02	0.49	0.03			0.38	0.09	0.68	0.01	0.03	3.1E-02	0.20	-0.05	0.44
MYBPH	0.03	-0.03	0.09	0.34	0.54	-2.0E-04	-0.08	-0.15	0.00	0.04		0.01	-0.05	0.08	0.64
NDRG1	-0.04	-0.28	0.20	0.74	0.85	0.01	-0.12	-0.40	0.15	0.39		-0.09	-0.34	0.16	0.48
P4HA1	-0.03	-0.41	0.35	0.88			-0.68	-1.18	-0.23	4.4E-03	0.02	-0.1	-0.25	-0.64	0.15
PDHX	-0.23	-0.66	0.20	0.29	0.52	-0.03	-0.07	-0.57	0.43	0.78		-0.24	-0.69	0.22	0.31
PGM5	0.36	0.20	0.53	1.9E-05	7.4E-04	0.06	0.04	-0.17	0.26	0.71		0.28	0.10	0.45	2.1E-03
POU2AF1	0.15	3.0E-04	0.29	0.05	0.12	0.01	0.12	-0.06	0.31	0.20		0.11	-0.04	0.26	0.16
PRAME	-0.01	-0.08	0.06	0.79	0.87	-0.01	0.07	-0.02	0.15	0.13		0.08	0.00	0.15	0.05

Supplementary Table 4. (continued)

Gene	Overall survival					Lymph node metastasis					Disease free survival				
	Univariate estimate	Estimate 95%CI	p-value	FDR	Ridge estimate ^a	Univariate estimate	Estimate 95%CI	p-value	FDR	Ridge estimate ^a	Univariate estimate	Estimate 95%CI	p-value	FDR	Ridge estimate ^a
PTPRB	0.27	-0.07 0.61	0.12	0.26	0.01	0.10	-0.27 0.49	0.59			0.19	-0.17 0.56	0.29	0.42	-1.9E-02
RGS5	0.33	0.09 0.58	0.01			0.37	0.02 0.74	0.05	0.07	0.1	0.39	0.13 0.66	0.00		
SCG5	0.02	-0.22 0.26	0.87			-0.31	-0.62 -0.03	0.04	0.07	-3.3E-02	-0.02	-0.27 0.22	0.85		
SELE	0.22	0.05 0.39	0.01	0.05	0.03	0.21	0.00 0.45	0.06			0.29	0.13 0.46	5.9E-04	0.01	0.06
SELP	0.28	0.12 0.43	4.9E-04	0.01	0.05	0.24	0.03 0.48	0.03			0.33	0.17 0.48	3.3E-05	1.3E-03	0.08
SERPINB2	-0.02	-0.14 0.10	0.77			0.21	0.05 0.39	0.02	0.04	0.1	-0.08	-0.22 0.05	0.23		
SERPINH1	0.07	-0.22 0.36	0.64			-0.56	-0.96 -0.19	4.1E-03	0.02	-0.1	-0.16	-0.43 0.12	0.26		
SLC5A12	-0.04	-0.13 0.05	0.36	0.55	-0.01	0.04	-0.07 0.16	0.43			0.05	-0.04 0.14	0.28	0.42	0.06
SPANXA	-0.01	-0.08 0.05	0.69	0.84	0.00	0.04	-0.05 0.12	0.40			0.01	-0.06 0.09	0.70	0.74	4.2E-02
SPOCK1	-0.05	-0.24 0.14	0.58			-0.32	-0.57 -0.09	0.01	0.03	-4.5E-02	-0.20	-0.40 0.00	0.05		
SPRR2G	0.02	-0.06 0.10	0.66	0.83	-3.7E-03	0.18	0.07 0.31	2.9E-03			-0.03	-0.12 0.06	0.51	0.61	-4.3E-02
SYNPO2	0.10	-0.05 0.25	0.20	0.39	1.5E-03	-0.04	-0.22 0.13	0.63			0.13	-0.03 0.29	0.11	0.24	7.0E-03
TANC2	-0.04	-0.39 0.31	0.83	0.87	-4.8E-03	-0.43	-0.87 -0.01	0.05			-0.37	-0.74 0.00	0.05	0.15	-0.07
TCL1A	0.20	0.08 0.31	1.0E-03	0.01	0.06	0.14	-0.01 0.29	0.08			0.17	0.05 0.30	0.01	0.03	0.06
TIMM8B	0.17	-0.18 0.52	0.33			0.32	-0.07 0.73	0.11	0.14	2.6E-02	0.20	-0.17 0.57	0.29		
TNNC1	0.05	-0.03 0.12	0.23	0.45	4.0E-03	-0.06	-0.15 0.03	0.22			0.05	-0.03 0.13	0.22	0.38	8.3E-03
TNXB	0.24	0.04 0.43	0.02	0.09	0.03	0.22	0.00 0.46	0.06			0.31	0.11 0.51	2.5E-03	0.02	0.06
TPM1	0.04	-0.15 0.24	0.67			-0.45	-0.73 -0.20	7.9E-04	0.01	-0.1	-0.07	-0.28 0.13	0.50		
TSPAN11	0.28	0.04 0.51	0.02	0.09	0.03	0.15	-0.17 0.47	0.36			0.26	-0.01 0.52	0.06	0.16	3.3E-02
VEGFA	-0.26	-0.51 -0.02	0.04	0.12	-0.04	-0.08	-0.39 0.22	0.59			-0.22	-0.48 0.05	0.11	0.24	-3.5E-02

^a Confidence intervals are not provided, because methodology to construct these is lacking for logistic ridge regression. In addition, they are likely uninformative (wide) due to collinearity in the variables.

Supplementary Table 5. Coefficients and p-values of clinical and pathological variables for integration with gene signatures

Variable name	Univariate overall survival			Multivariate overall survival		Univariate disease-free survival	
	p-value	Coefficient		p-value	Coefficient	p-value	Coefficient
ECOG (0 ^a /1)	0.14	0.59				0.92	-0.05
Age	0.001	0.04		9.50E-04	0.05	0.69	0.005
ACE27 (none ^a /mild/moderate+severe)	0.02	0.93	1.16			0.28	0.46
Sex (male ^a /female)	0.1	0.51				0.64	0.15
PackYears	0.005	0.02		0.003	0.02	0.32	0.007
pTNM (1+2 ^a vs. 3+4)	0.44	0.24		0.29	0.33	0.39	0.29
pCompVar (negative ^a /positive)	7.00E-06	1.4				7.00E-05	1.3

^a. Reference category

Supplementary Table 6. Remark criteria checklist

Item to be reported		
Introduction		
1	State the marker examined, the study objectives, and any pre-specified hypotheses.	X
Material and methods		
Patients		
2	Describe the characteristics (e.g., disease stage or co-morbidities) of the study patients, including their source and inclusion and exclusion criteria.	X
3	Describe treatments received and how chosen (e.g., randomized or rule-based).	X
Specimen characteristics		
4	Describe type of biological material used (including control samples) and methods of preservation and storage.	X
Assay methods		
5	Specify the assay method used and provide (or reference) a detailed protocol, including specific reagents or kits used, quality control procedures, reproducibility assessments, quantitation methods, and scoring and reporting protocols. Specify whether and how assays were performed blinded to the study endpoint.	X
Study design		
6	State the method of case selection, including whether prospective or retrospective and whether stratification or matching (e.g., by stage of disease or age) was used. Specify the time period from which cases were taken, the end of the follow-up period, and the median follow-up time.	X
7	Precisely define all clinical endpoints examined.	X
8	List all candidate variables initially examined or considered for inclusion in models.	X
9	Give rationale for sample size; if the study was designed to detect a specified effect size, give the target power and effect size.	X
Statistical analysis methods		
10	Specify all statistical methods, including details of any variable selection procedures and other model-building issues, how model assumptions were verified, and how missing data were handled.	X
11	Clarify how marker values were handled in the analyses; if relevant, describe methods used for cutpoint determination.	X
Results		
Data		
12	Describe the flow of patients through the study, including the number of patients included in each stage of the analysis (a diagram may be helpful) and reasons for dropout. Specifically, both overall and for each subgroup extensively examined report the numbers of patients and the number of events.	X
13	Report distributions of basic demographic characteristics (at least age and sex), standard (disease-specific) prognostic variables, and tumor marker, including numbers of missing values.	X
Analysis and presentation		
14	Show the relation of the marker to standard prognostic variables.	X
15	Present univariable analyses showing the relation between the marker and outcome, with the estimated effect (e.g., hazard ratio and survival probability). Preferably provide similar analyses for all other variables being analyzed. For the effect of a tumor marker on a time-to-event outcome, a Kaplan-Meier plot is recommended.	X
16	For key multivariable analyses, report estimated effects (e.g., hazard ratio) with confidence intervals for the marker and, at least for the final model, all other variables in the model.	X
17	Among reported results, provide estimated effects with confidence intervals from an analysis in which the marker and standard prognostic variables are included, regardless of their statistical significance.	X
18	If done, report results of further investigations, such as checking assumptions, sensitivity analyses, and internal validation.	X
Discussion		
19	Interpret the results in the context of the pre-specified hypotheses and other relevant studies; include a discussion of limitations of the study.	X
20	Discuss implications for future research and clinical value.	X

Supplementary Table 7. Housekeeping gene performance

Housekeeping gene	Correlation coefficient					SD ^a
	GAPDH	GUSB	RPL4	RPLP0	mean-Ct target genes ^b	
GAPDH	1	0.77	0.82	0.83	0.69	1.17
GUSB	0.77	1	0.72	0.71	0.77	0.94
RPL4	0.82	0.72	1	0.87	0.67	1.05
RPLP0	0.83	0.71	0.87	1	0.65	0.98

^a. Standard deviation of housekeeping gene across all samples.
^b. Correlation of Ct-value of housekeeping gene and average Ct-value of all target genes (n=60).

Supplementary Table 8. Assessment of performance of the gene signature in relevant subgroups by integrated area-under-the-curve (iAUC)

Subgroup	OS			DFS			n
	iAUC	95% CI		iAUC	95% CI		
CompVar: 0	0.71	0.65	0.76	0.65	0.61	0.68	79
CompVar: 1	0.58	0.51	0.65	0.62	0.55	0.7	38
Age<70	0.64	0.59	0.7	0.62	0.57	0.68	88
Age>=70	0.56	0.48	0.66	0.76	0.7	0.82	37
PackYears < median	0.61	0.54	0.69	0.7	0.65	0.75	59
PackYears >= median	0.54	0.48	0.62	0.54	0.47	0.63	66
Female	0.58	0.51	0.67	0.56	0.49	0.63	53
Male	0.63	0.56	0.69	0.64	0.58	0.72	72
pTNM: 1 or 2	0.6	0.52	0.68	0.53	0.45	0.64	43
pTNM: 3 or 4	0.63	0.57	0.69	0.63	0.57	0.7	82
ACE27: 0-1	0.66	0.6	0.73	0.68	0.63	0.75	77
ACE27: 2-3	0.65	0.57	0.74	0.56	0.49	0.63	48
Treatment surgery only	0.51	0.43	0.61	0.69	0.65	0.71	60
Treatment surgery + adjuvant	0.67	0.61	0.73	0.65	0.58	0.73	65

REFERENCES

1. Ferlay J, Soerjomataram I, Dikshit R, et al. Cancer incidence and mortality worldwide: sources, methods and major patterns in GLOBOCAN 2012. *Int J Cancer* 2015; 136(5): E359-86.
2. Braakhuis BJ, Leemans CR, Visser O. Incidence and survival trends of head and neck squamous cell carcinoma in the Netherlands between 1989 and 2011. *Oral Oncol* 2014; 50(7): 670-5.
3. Gillison ML, Chaturvedi AK, Anderson WF, Fakhry C. Epidemiology of Human Papillomavirus-Positive Head and Neck Squamous Cell Carcinoma. *J Clin Oncol* 2015; 33(29): 3235-42.
4. Castellsague X, Alemany L, Quer M, et al. HPV Involvement in Head and Neck Cancers: Comprehensive Assessment of Biomarkers in 3680 Patients. *J Natl Cancer Inst* 2016; 108(6): djv403.
5. Braakhuis BJ, Snijders PJ, Keune WJ, et al. Genetic patterns in head and neck cancers that contain or lack transcriptionally active human papillomavirus. *J Natl Cancer Inst* 2004; 96(13): 998-1006.
6. O'Sullivan B, Huang SH, Su J, et al. Development and validation of a staging system for HPV-related oropharyngeal cancer by the International Collaboration on Oropharyngeal cancer Network for Staging (ICON-5): a multicentre cohort study. *Lancet Oncol* 2016; 17(4): 440-51.
7. Brierley JDG, M. K.; Wittekind, C., eds. *TNM Classification of Malignant Tumours*. 8th Edition ed. Hoboken: Wiley-Blackwell; 2016.
8. Chinn SB, Myers JN. Oral Cavity Carcinoma: Current Management, Controversies, and Future Directions. *J Clin Oncol* 2015; 33(29): 3269-76.
9. Leemans CR, Braakhuis BJ, Brakenhoff RH. The molecular biology of head and neck cancer. *Nat Rev Cancer* 2011; 11(1): 9-22.
10. Chung CH, Parker JS, Ely K, et al. Gene expression profiles identify epithelial-to-mesenchymal transition and activation of nuclear factor-kappaB signaling as characteristics of a high-risk head and neck squamous cell carcinoma. *Cancer Res* 2006; 66(16): 8210-8.
11. De Cecco L, Bossi P, Locati L, Canevari S, Licitra L. Comprehensive gene expression meta-analysis of head and neck squamous cell carcinoma microarray data defines a robust survival predictor. *Ann Oncol* 2014; 25(8): 1628-35.
12. Lohavanichbutr P, Mendez E, Holsinger FC, et al. A 13-gene signature prognostic of HPV-negative OSCC: discovery and external validation. *Clin Cancer Res* 2013; 19(5): 1197-203.
13. Jung AC, Job S, Ledrappier S, et al. A poor prognosis subtype of HNSCC is consistently observed across methylome, transcriptome, and miRNome analysis. *Clin Cancer Res* 2013; 19(15): 4174-84.
14. Tan PK, Downey TJ, Spitznagel EL, Jr., et al. Evaluation of gene expression measurements from commercial microarray platforms. *Nucleic Acids Res* 2003; 31(19): 5676-84.
15. Roepman P, Kemmeren P, Wessels LF, Slootweg PJ, Holstege FC. Multiple robust signatures for detecting lymph node metastasis in head and neck cancer. *Cancer Res* 2006; 66(4): 2361-6.
16. Roepman P, Wessels LF, Kettelarij N, et al. An expression profile for diagnosis of lymph node metastases from primary head and neck squamous cell carcinomas. *Nat Genet* 2005; 37(2): 182-6.
17. van Hooff SR, Leusink FK, Roepman P, et al. Validation of a gene expression signature for assessment of lymph node metastasis in oral squamous cell carcinoma. *J Clin Oncol* 2012; 30(33): 4104-10.
18. Schilling C, Stoeckli SJ, Haerle SK, et al. Sentinel European Node Trial (SENT): 3-year results of sentinel node biopsy in oral cancer. *Eur J Cancer* 2015; 51(18): 2777-84.
19. Cancer Genome Atlas N. Comprehensive genomic characterization of head and neck squamous cell carcinomas. *Nature* 2015; 517(7536): 576-82.
20. McShane LM, Altman DG, Sauerbrei W, et al. Reporting recommendations for tumor marker prognostic studies. *J Clin Oncol* 2005; 23(36): 9067-72.
21. Smeets SJ, Hesselink AT, Speel EJ, et al. A novel algorithm for reliable detection of human papillomavirus in paraffin embedded head and neck cancer specimen. *Int J Cancer* 2007; 121(11): 2465-72.
22. Ritchie ME, Phipson B, Wu D, et al. limma powers differential expression analyses for RNA-sequencing and microarray studies. *Nucleic Acids Res* 2015; 43(7): e47.
23. Livak KJ, Schmittgen TD. Analysis of relative gene expression data using real-time quantitative PCR and the 2(-Delta Delta C(T)) Method. *Methods* 2001; 25(4): 402-8.
24. Goeman JJ, Oosting J, Cleton-Jansen AM, Anninga JK, van Houwelingen HC. Testing association of a pathway with survival using gene expression data. *Bioinformatics* 2005; 21(9): 1950-7.

25. Goeman JJ, van de Geer SA, de Kort F, van Houwelingen HC. A global test for groups of genes: testing association with a clinical outcome. *Bioinformatics* 2004; 20(1): 93-9.
26. Benjamini Y, Hochberg Y. Controlling the False Discovery Rate - a Practical and Powerful Approach to Multiple Testing. *J R Stat Soc B* 1995; 57(1): 289-300.
27. Alkureishi LW, Ross GL, Shoaib T, et al. Sentinel node biopsy in head and neck squamous cell cancer: 5-year follow-up of a European multicenter trial. *Ann Surg Oncol* 2010; 17(9): 2459-64.
28. Den Toom IJ, Heuveling DA, Flach GB, et al. Sentinel node biopsy for early-stage oral cavity cancer: the VU University Medical Center experience. *Head Neck* 2015; 37(4): 573-8.
29. Civantos FJ, Zitsch RP, Schuller DE, et al. Sentinel lymph node biopsy accurately stages the regional lymph nodes for T1-T2 oral squamous cell carcinomas: results of a prospective multi-institutional trial. *J Clin Oncol* 2010; 28(8): 1395-400.
30. Leusink FK, van Es RJ, de Bree R, et al. Novel diagnostic modalities for assessment of the clinically node-negative neck in oral squamous-cell carcinoma. *Lancet Oncol* 2012; 13(12): e554-61.
31. Pramana J, Pimentel N, Hofland I, et al. Heterogeneity of gene expression profiles in head and neck cancer. *Head Neck* 2007; 29(12): 1083-9.
32. Johnson WE, Li C, Rabinovic A. Adjusting batch effects in microarray expression data using empirical Bayes methods. *Biostatistics* 2007; 8(1): 118-27.
33. Rickman DS, Millon R, De Reynies A, et al. Prediction of future metastasis and molecular characterization of head and neck squamous-cell carcinoma based on transcriptome and genome analysis by microarrays. *Oncogene* 2008; 27(51): 6607-22.
34. Onken MD, Winkler AE, Kanchi KL, et al. A surprising cross-species conservation in the genomic landscape of mouse and human oral cancer identifies a transcriptional signature predicting metastatic disease. *Clin Cancer Res* 2014; 20(11): 2873-84.
35. Thurlow JK, Pena Murillo CL, Hunter KD, et al. Spectral clustering of microarray data elucidates the roles of microenvironment remodeling and immune responses in survival of head and neck squamous cell carcinoma. *J Clin Oncol* 2010; 28(17): 2881-8.
36. Winter SC, Buffa FM, Silva P, et al. Relation of a hypoxia metagene derived from head and neck cancer to prognosis of multiple cancers. *Cancer Res* 2007; 67(7): 3441-9.
37. Chen C, Mendez E, Houck J, et al. Gene expression profiling identifies genes predictive of oral squamous cell carcinoma. *Cancer Epidemiol Biomarkers Prev* 2008; 17(8): 2152-62.
38. Sobin LH, M.K.; Wittekind, C.; eds. *TNM Classification of Malignant Tumours*. 7th Edition ed. Hoboken: Wiley-Blackwell; 2009.
39. Batsakis JG. Surgical excision margins: a pathologist's perspective. *Adv Anat Pathol* 1999; 6(3): 140-8.
40. van den Brekel MW, Lodder WL, Stel HV, Bloemena E, Leemans CR, van der Waal I. Observer variation in the histopathologic assessment of extranodal tumor spread in lymph node metastases in the neck. *Head Neck* 2012; 34(6): 840-5.
41. Oken MM, Creech RH, Tormey DC, et al. Toxicity and response criteria of the Eastern Cooperative Oncology Group. *Am J Clin Oncol* 1982; 5(6): 649-55.
42. Piccirillo JF, Tierney RM, Costas I, Grove L, Spitznagel EL, Jr. Prognostic importance of comorbidity in a hospital-based cancer registry. *JAMA* 2004; 291(20): 2441-7.
43. Schemper M, Smith TL. A note on quantifying follow-up in studies of failure time. *Control Clin Trials* 1996; 17(4): 343-6.
44. Heagerty PJ, Lumley T, Pepe MS. Time-dependent ROC curves for censored survival data and a diagnostic marker. *Biometrics* 2000; 56(2): 337-44.
45. Jiang B, Zhang XG, Cai TX. Estimating the confidence interval for prediction errors of support vector machine classifiers. *J Mach Learn Res* 2008; 9: 521-40.
46. Jiang W, Varma S, Simon R. Calculating confidence intervals for prediction error in microarray classification using resampling. *Stat Appl Genet Mol Biol* 2008; 7(1): Article8.
47. Wahl S, Boulesteix AL, Zierer A, Thorand B, van de Wiel MA. Assessment of predictive performance in incomplete data by combining internal validation and multiple imputation. *BMC Med Res Methodol* 2016; 16(1): 144.

